www.springer.com/41230
https://doi.org/10.1007/s41230-026-5217-z
Special Review CHINA FOUNDRY
Vol. 23 No. 2 March 2026

Hot tearing of cast aluminium alloys: A critical review

You-jie Guo, Fang-zhou Qi, Yi-hao Wang, Guang-ling Wei, *Liang Zhang, and Guo-hua Wu
School of Materials Science and Engineering, Shanghai Jiao Tong University, Shanghai 200240, China

Abstract: Cast aluminum (Al) alloys, owing to their low density and high specific strength, offer significant advantages in the fabrication of complex, large-scale, or monolithic structural components across civilian, defense, and military sectors that are weight-sensitive, including transportation, aerospace, and underwater weaponry. However, a substantial portion of these alloys often exhibit pronounced hot tearing susceptibility (HTS) during casting, which not only detrimentally affects the quality and efficiency of industrial production but also limits their further development in high-tech applications. Therefore, a comprehensive and profound understanding of hot tearing behavior in cast Al alloys is essential. This review first analyzes the formation mechanisms of hot tearing, encompassing strength theory, liquid film theory, intergranular bridging theory, solidification shrinkage compensation theory, and relevant models, as well as the key factors governing its occurrence, including alloy composition, grain structure, casting parameters, and inclusions. It then introduces current research methods, ranging from simple evaluation and physical parameter-based approaches to in situ observation and numerical simulation, followed by a summary of newly proposed hot tearing criteria. Finally, it discusses the remaining scientific challenges and outlines future research directions. Particular emphasis is placed on recent advances in the hot tearing of cast Al alloys over the past decade.

Keywords: aluminium alloys; hot tearing; casting; hot tearing mechanisms; hot tearing criteria; numerical simulation

CLC numbers: TG146.21 **Document code:** A **Article ID:** 1672-6421(2026)02-117-22

1 Introduction

Aluminum (Al) alloy castings have been widely used in automotive, aerospace, marine, and other structural component applications due to their low density, high specific strength, excellent corrosion resistance, and good recyclability[1]. Their capacity to produce complex, large-scale, or integrated components through various casting processes makes them highly attractive for both industrial mass production and advanced lightweight design[2]. However, casting is inherently prone to solidification defects, among which hot tearing (also referred to as hot cracking, hot shortness, or solidification cracking) is considered one of the most catastrophic and irreversible[3]. It typically comprises a primary tear accompanied by numerous minor branches that propagate along intergranular paths, with the fracture surface exhibiting a dendritic morphology[4]. Despite continued alloying and process optimization, hot tearing remains a prevalent and unresolved issue. It severely compromises the structural integrity and production reliability of cast Al alloy castings, posing a major challenge to both industrial application and fundamental alloy design[5]. Therefore, a deep understanding of hot tearing mechanisms and the effective mitigation of hot tearing susceptibility (HTS) are imperative for improving the ultimate performance of cast Al alloys.

Hot tearing in cast Al alloys occurs during the late stages of solidification, within the temperature range above the solidus yet below the dendritic coherency temperature, wherein the alloy exists in a semi-solid state comprising a developing solid skeleton and interdendritic liquid[6]. As solidification proceeds, the semi-solid structure gradually acquires mechanical strength, making it vulnerable to thermally and mechanically induced strains/stresses arising from solidification shrinkage, thermal contraction, and external constraints. When these strains/stresses exceed the local mechanical limit of the semi-solid network,

*Liang Zhang
Male, born in 1985, Ph. D. Research interests: Development and precision forming of high-performance light alloy materials.
E-mail: liangzhang08@sjtu.edu.cn
Received: 2025-09-10; Revised: 2025-10-22; Accepted: 2025-11-20

cracks may initiate along interdendritic liquid films or at dendrite-bridging fracture sites[7]. Such cracks are most likely to form in regions where shrinkage is constrained, particularly at hot spots, areas that solidify last and experience significant thermal gradients. The subsequent evolution of cracks depends on the ability of the remaining liquid to compensate for local shrinkage and fill the developing cavities[8]. However, as permeability decreases and liquid feeding becomes insufficient, cracks cannot heal and become permanent[9, 10]. Therefore, HTS is thus governed by a complex interplay between the evolving mechanical integrity of the semi-solid skeleton and the feeding capacity of the interdendritic liquid, both of which are strongly influenced by alloy composition, grain morphology, solidification range, and cooling conditions.

Building upon the comprehensive reviews by Eskin[6] and Li[7], which established the foundational understanding of hot tearing in cast Al alloys, this review provides an updated and state-of-the-art perspective focusing on developments over the past decade. The current insights into hot tearing formation mechanisms and key influencing factors are systematically analyzed, the emerging research methods are summarized, and the latest hot tearing criteria are critically evaluated. Particular emphasis is placed on novel experimental and modeling approaches that enhance predictive capabilities. By integrating these developments, this review aims to bridge existing knowledge gaps and outline promising directions for future research in mitigating HTS.

2 Hot tearing mechanisms

2.1 Strength theory

Strength theory suggests that hot tearing occurs during the final stages of solidification, when a substantial solid skeleton has formed and begins to contract as temperature decreases. If this contraction is constrained by the mold, stresses or strains develop. Once these stresses exceed the mechanical strength or deformation limits of the alloy at the given temperature, cracks initiate to release the accumulated stress. Extensive studies have demonstrated that hot tearing arises in the mushy zone, where interdendritic liquid films coexist with a rapid loss of strength and ductility. Experimental observations indicate that the tensile strength and plasticity of semi-solid alloys drop sharply within a narrow temperature range above the solidus, creating a critical vulnerability window for cracking. Strength theory therefore highlights the interplay between stress accumulation from solidification shrinkage and the evolving mechanical limits of the semi-solid network, explaining why hot tearing predominantly initiates near or slightly above the solidus[11, 12]. Nonetheless, this theory has limitations: its reliance on a simplified critical strength threshold cannot fully capture complex stress states, and it overlooks microstructural features and the essential role of liquid feeding in hot tearing formation.

2.2 Liquid film theory

Liquid film theory posits that hot tearing occurs when interdendritic liquid films become increasingly constrained by the growing dendritic skeleton, which impedes liquid feeding and shrinkage compensation. At elevated temperatures, weak grain bonding causes localized tensile stresses to concentrate on the liquid films, leading to separation of adjacent grains and crack initiation. The cracking process can be divided into three stages: (1) Initially, small grains are surrounded by liquid films connected to the bulk liquid. (2) As grains grow and contact each other, liquid flow is restricted, and surface tension generates an additional pressure on the liquid films to counter external stresses. (3) When applied stresses exceed the maximum pressure sustainable by the liquid films, rupture occurs, grains separate, and cracks propagate. The thickness and persistence of the liquid film are influenced by low-melting eutectic phases, and crack propagation depends on whether tensile stresses surpass the surface tension[13-15]. This theory systematically elucidates the role of the liquid films in hot tearing, emphasizing that restricted feeding and localized stress concentration are critical factors in crack formation. However, it neglects the mechanical behavior of the solid phase and oversimplifies the complex interplay of liquid feeding and shrinkage compensation.

2.3 Intergranular bridging theory

Intergranular bridging theory proposes that growing dendrites form bridges at grain boundaries near the end of solidification, establishing cohesion that can approach or match the intrinsic strength of the grains, thereby resisting hot tearing[16-18]. The solidification process is divided into four zones: the quasi-liquid zone, feeding zone, interdendritic separation zone, and interdendritic bridging zone. First, sparse dendrites exist in a primarily liquid matrix (quasi-liquid zone). As nucleation and dendrite growth progress, feeding occurs between grains. Further growth leads to interdendritic separation in poorly fed regions, while well-fed regions develop interdendritic bridges that enhance grain boundary cohesion, significantly increasing fracture strength beyond the critical stress predicted by liquid film theory. Hot tearing is thus attributed to the disruption of these bridges when solidification shrinkage is constrained. Faster dendrite growth and earlier grain contact promote extensive bridging, improving grain boundary strength and reducing HTS[15, 19-21]. However, this theory neglects the influence of liquid feeding during solidification shrinkage, and quantifying parameters such as bridge strength remains challenging.

2.4 Solidification shrinkage compensation theory

Solidification shrinkage compensation theory divides the solidification process into four stages: the quasi-liquid stage, feeding stage, non-feeding stage, and grain-bridging stage. During the quasi-liquid stage, the dendritic skeleton is minimal, resulting in low strength, high ductility, and efficient liquid feeding, making hot cracking unlikely. As solidification progresses into the feeding and non-feeding stages, the dendritic network develops, strength increases, and ductility drops to a minimum. During these low-plasticity stages, thermally

induced contraction and solidification shrinkage, when mechanically constrained, can lead to intergranular separation. If liquid metal flows in to heal microvoids, cracking is avoided; otherwise, microvoids grow along interdendritic liquid films, eventually forming hot cracks. At the final grain-bridging stage, continued cooling promotes grain contact and strengthens grain boundaries, increasing both strength and ductility. However, if the contraction stress exceeds the strength of these grain bridges, small interdendritic cavities can coalesce into continuous hot cracks[22, 23]. Despite its explanatory power, this theory oversimplifies the mechanisms of liquid flow and feeding, limiting its direct quantitative predictive capability.

Beyond the four classical theories, alternative models, including impact stress, cohesion loss, and percolation theories, have been proposed to explain hot tearing[24–26]. Fundamentally, hot tearing involves a two-stage process: first, thermal and solidification shrinkage stresses exceed the mechanical limits of the mushy zone's solid skeleton, leading to micropore nucleation; second, the propagation or healing of these micropores depends on the efficiency of interdendritic liquid feeding[27]. The dominant cracking mechanism also varies with alloy composition: higher-solute alloys typically fail via liquid film rupture, whereas lower-solute alloys fail through solid bridge fracture, which exhibits mixed brittle-ductile features. Consequently, crack propagation is governed by solid fraction, microstructure, and alloy composition. Collectively, these theories provide a comprehensive framework for understanding the formation of hot tearing in casting processes.

3 Key factors determining hot tearing

3.1 Alloy composition

Pure metals are generally resistant to hot tearing because they solidify almost isothermally. In contrast, alloys exhibit a finite solidification temperature range. The wider this range, particularly during the final stages of solidification, the longer the alloy remains in a semi-solid state, thereby increasing the susceptibility to hot tearing[6]. For simple binary alloys, the HTS typically follows a characteristic "Λ-shaped" dependence on solute content, which is closely associated with the freezing range and the amount of eutectic liquid[2, 28], as illustrated in Fig. 1(a)[2]. At low solute concentrations, HTS rises with increasing solute content due to the extended freezing range. However, as solute content further increases and eutectic phases form, the residual liquid generated at the late stage of solidification can compensate for shrinkage and heal micropores, while the enhanced melt fluidity also contributes to reducing HTS[29, 30]. Since eutectic reactions occur nearly isothermally, alloys with eutectic compositions usually show very low HTS. More recently, Hu et al.[31, 32] reported that in dual-ternary eutectic systems such as Al-6Mg-*x*Si and Mg-4Ce-*x*Al, the combined effects of dual-ternary eutectic reactions and secondary phase evolution result in a double-peak hot tearing trend, as these alloys experience two distinct eutectic reaction plateaus during solidification. This finding further substantiates the relationship among the freezing range, residual liquid, and hot tearing behavior. For ternary and more complex multi-component alloys, the dependence of HTS on composition is often represented by contour maps generated using specific criteria or indicators, where multiple susceptibility peaks may emerge[33–35].

In addition to these compositional effects on the solidification range and eutectic reactions, the solidification shrinkage coefficient is another crucial thermophysical factor governing HTS. The shrinkage coefficient, which quantifies the volumetric change during the liquid-to-solid transition, varies significantly among different Al alloy systems. For instance, Al-Si alloys exhibit relatively low solidification shrinkage (~3% for Al-7Si at 600 °C) due to the high Si content and eutectic solidification behavior, whereas Al-Cu and Al-Li alloys experience pronounced volumetric contraction (~7.5% for Al-4Cu and ~7% for Al-3Li at 600 °C, respectively) owing to the large density difference between the solid and liquid phases[2, 3]. A larger shrinkage coefficient increases the feeding demand and intensifies tensile stress accumulation within the semi-solid network, thereby aggravating HTS, while smaller shrinkage values, typical of high-Si or eutectic-rich alloys, help alleviate feeding deficiency and mitigate cracking[6]. Therefore, variations in shrinkage coefficients among different alloy compositions provide an important thermophysical explanation for their distinct HTS.

The solute equilibrium partition coefficient (k) plays a fundamental role in solute segregation during solidification. A smaller k value indicates a stronger tendency for solute enrichment at grain boundaries or interdendritic regions[36]. Such segregation suppresses or delays grain boundary bridging, preventing the formation of a continuous alloy skeleton. Consequently, under tensile stress, hot tearing is more prone to occur[37]. Back diffusion also exerts a significant influence on hot tearing. For solutes with relatively large k values or diffusion coefficients (D), solute atoms can readily diffuse from interdendritic liquid into the solid under the typical slow cooling conditions of casting, resulting in pronounced back diffusion. This process is often described by the back-diffusion parameter (α'), defined as[38]:

$$\alpha' = \alpha\left[1-\exp\left(-\frac{1}{\alpha}\right)\right]-\frac{1}{2}\exp\left(-\frac{1}{2\alpha}\right) \quad (1)$$

$$\alpha = \frac{4Dt}{\lambda^2} \quad (2)$$

where α represents the dimensionless solidification time, D is the diffusion coefficient of solute in solid dendrites, t denotes the local solidification time, and λ is the secondary dendrite arm spacing. An increase in α', i.e., the enhanced solute diffusion into dendrites, reduces the degree of solute segregation at grain boundaries and thereby mitigates HTS. In practice, the increase in α' suppresses the peak of the "Λ-shaped" curve and shifts it toward higher solute contents. The effects of k and α' are particularly pronounced in Al-Mg alloys. Geng et al.[39, 40] reported that Al-Mg alloys can exhibit superior resistance to solidification cracking compared with Al-Cu alloys, despite

their wider freezing range. Even under rapid cooling conditions without back diffusion, extensive dendrite coalescence occurs at earlier solidification stages in Al-Mg alloys, which enhances resistance to hot tearing. Meanwhile, Liu et al.[38, 41] further demonstrated that Al-Mg alloys exhibit significant back diffusion, which reduces solute segregation at grain boundaries and interdendritic regions, thereby lowering HTS [Fig. 1(b)][28, 41], even though these alloys solidify over a relatively wide temperature range.

Both the k and α' regulate solute redistribution during solidification, and thereby dictate the timing and extent of dendrite coalescence. Beyond solute partitioning, however, the wettability between solid and liquid phases further determines whether interdendritic liquid persists as a continuous film or is effectively bridged, thus exerting a decisive influence on HTS. Studies have shown that the degree of brittleness during hot tearing is strongly related to the dihedral angle (2θ), which can be expressed as[42]:

$$\gamma_{SS} = 2(\cos\theta)\gamma_{SL} \quad (3)$$

where γ_{SL} is the solid/liquid interfacial energy and γ_{SS} is the solid/solid interfacial energy. Assuming grain misorientation can be neglected, the 2θ is primarily governed by the balance of these interfacial energies. In general, small values of 2θ correspond to higher HTS because they promotes the formation of continuous liquid films covering adjacent grain surfaces, which delay grain boundary bridging and hinder early coalescence. By contrast, larger values of 2θ favor liquid channel disconnection and solid-solid contact, facilitating the establishment of a coherent dendritic skeleton capable of resisting tensile stress[42, 43], as shown in Fig. 1(c).

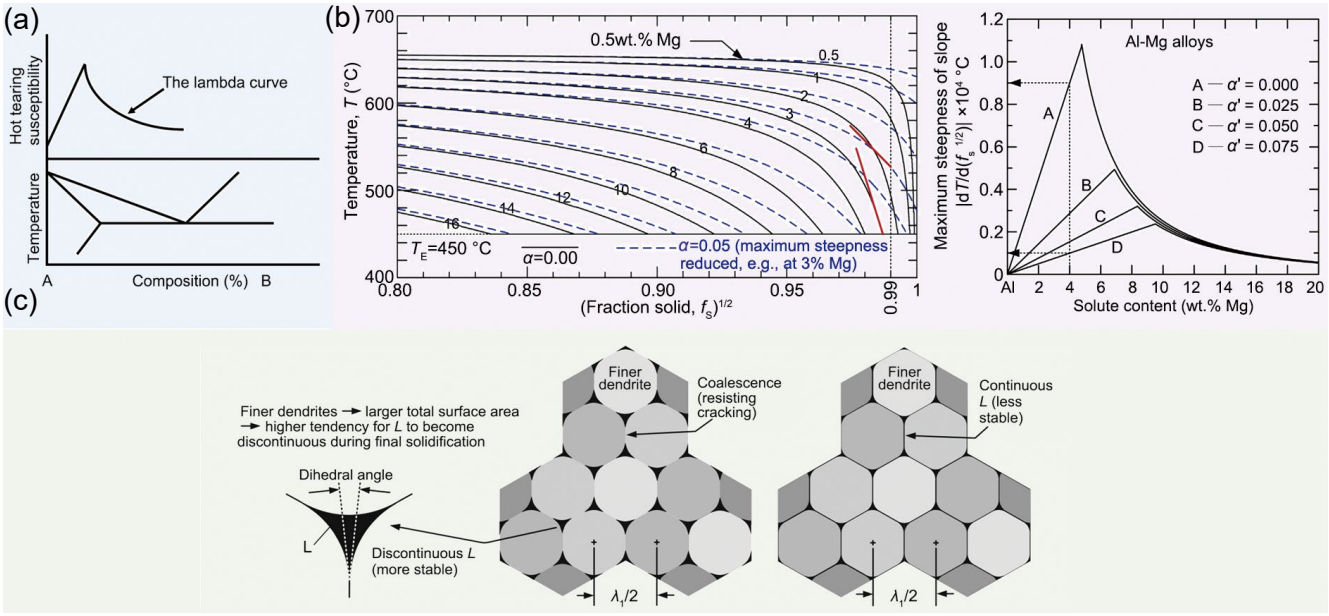

Fig. 1: Influence of alloy composition on HTS: (a) solidification temperature range with corresponding Λ-shaped curve[2]; (b) equilibrium partition coefficient k and back-diffusion parameter α' in Al-Mg alloys[28, 41]; (c) dihedral angle 2θ[43]

3.2 Grain structure

Grain morphology plays a decisive role in determining the HTS of alloys. Compared with columnar grains, equiaxed grains are generally considered beneficial because their random crystallographic orientations and globular morphologies promote intergranular bridging and create more tortuous crack-propagation paths. These features improve interdendritic feeding efficiency and delay crack opening. In contrast, columnar grains with elongated morphologies tend to form aligned boundaries and straight channels along the solidification direction, which not only restrict interdendritic feeding paths but also facilitate crack initiation and propagation along weakly bonded boundaries[7, 9]. Moreover, crystallographic alignment further modulates HTS. Preferentially oriented grains form coherent interfaces and directional solidification skeletons, which intensify stress concentration and provide continuous crack paths, thereby exacerbating hot tearing. Conversely, the orientation diversity typical of equiaxed grains enhances intergranular mismatch and increases resistance to crack propagation[44]. Thus, both grain morphology and orientation uniformity act synergistically to balance feeding capability and resistance to crack initiation and propagation, thereby, ultimately controlling HTS.

Grain refinement is widely acknowledged as an effective strategy to mitigate HTS, as it modifies both the thermal contraction behavior and mechanical response during solidification[45-60]. First, finer grains lower the temperature at which linear contraction occurs and reduce the overall contraction magnitude, thereby diminishing the driving force for crack formation. Second, the abundance of fine grains enhances strain accommodation via mechanisms such as grain rotation and boundary sliding, improving the capacity of the semi-solid network to withstand deformation without fracture. Third, refinement shortens interdendritic feeding channels while simultaneously increasing the number of bridging points

between adjacent grains, both of which facilitate liquid feeding and hinder crack opening. Furthermore, the higher grain boundary density of refined structures enlarges the total liquid film area, enabling more uniform stress distribution across the semi-solid skeleton [Fig. 2(a)][43]. In practice, grain refinement in cast Al alloys is commonly achieved by the addition of potent refiners such as Sc, Zr, and Ti, which promote heterogeneous nucleation and restrict dendrite growth[61–63]. It is worth noting, however, as emphasized by Kou[43], that the reduction in HTS through grain refinement arises primarily from accelerated grain coalescence rather than improved liquid feeding or permeability.

While grain refinement is generally advantageous, excessive refinement can paradoxically increase HTS[43]. When grains become ultrafine and packed, solute enrichment at grain interfaces impedes mutual growth and delays coalescence. In the end of solidification, ultrafine grains frequently assume globular or cellular equiaxed morphologies instead of dendritic ones. Such morphologies trap the limited interdendritic liquid, allowing continuous liquid films to persist along grain boundaries and further delaying solid bridging. Moreover, the absence of long dendrite arms prevents effective interlocking between neighboring grains, thereby reducing resistance to cracking. Finally, networks of ultrafine grains are associated with low permeability, which aggravates feeding difficulties. Thus, the mechanisms underlying over-refinement extend beyond the low-permeability explanation and are more fundamentally rooted in delayed coalescence and insufficient dendritic interconnection [Fig. 2(b)][43].

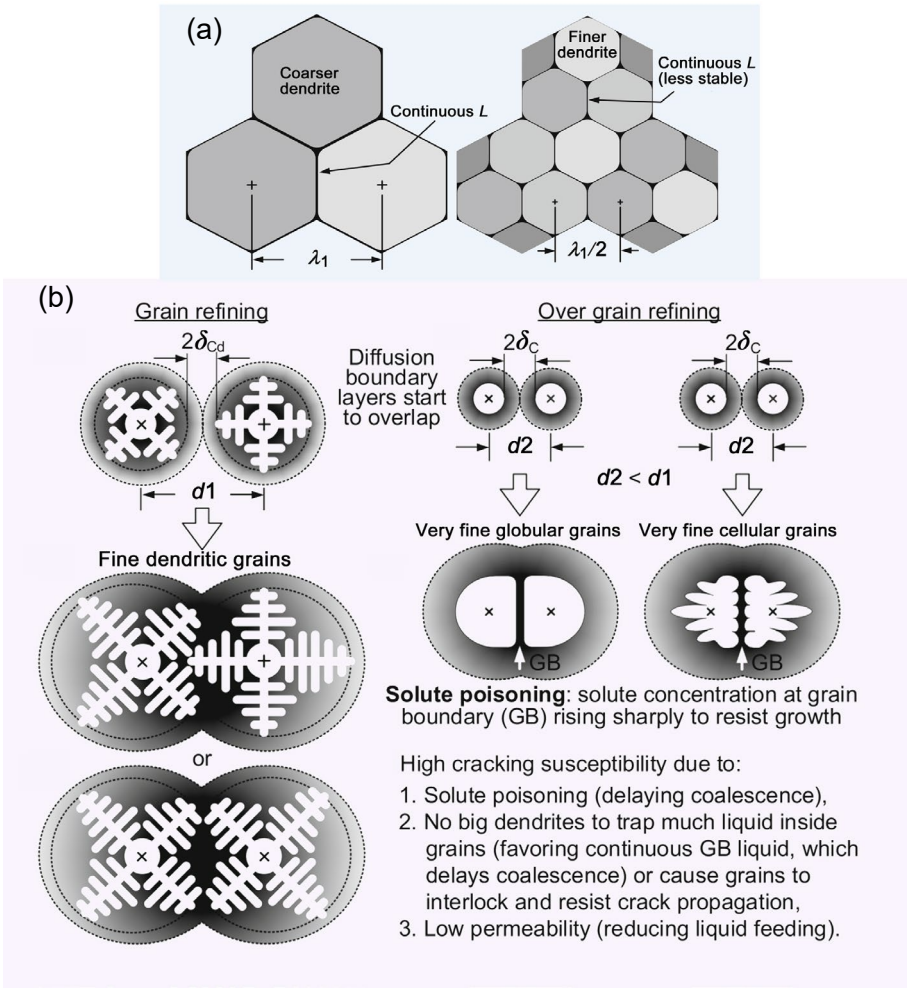

Fig. 2: Influence of grain refinement on HTS[43]: (a) moderate grain refinement reduces HTS; (b) over grain refinement increases HTS with underlying mechanisms

3.3 Casting parameters

The influence of pouring temperature on HTS is complex and often exhibits a non-monotonic trend. A moderate range of pouring temperatures generally reduces HTS, whereas temperatures that are excessively low or high tend to aggravate cracking[6, 7, 9]. This phenomenon is closely associated with the concept of superheat, defined as the extent to which the molten alloy temperature exceeds its liquidus. At moderate levels of superheat, enhanced melt fluidity and reduced cooling rates promote a more uniform temperature distribution throughout the casting. Such conditions narrow the solidification range, lower the solidification shrinkage rate, and alleviate localized stress concentrations, thereby reducing HTS[64, 65]. In addition, higher pouring temperatures can help dissipate localized hot spots, further decreasing the risk of hot tearing. Nevertheless, excessive superheat may have adverse consequences, as shown in Fig. 3(a). The prolonged presence of liquid films at grain boundaries delays grain coalescence, while steep temperature

gradients promote columnar dendritic growth, which is more susceptible to hot tearing compared with equiaxed structures. Moreover, it should be emphasized that excessively elevated pouring temperatures can significantly increase the oxidation tendency of certain cast Al alloys. Wang et al.[66] demonstrated that in Al-Li alloys, high pouring temperatures promote the formation of abundant Li-containing inclusions, which in turn intensify HTS. In addition, an excessively low pouring temperature increases the viscosity and reduces the fluidity of the molten alloy, which compromises mold-filling capacity and hampers feeding, thereby increasing the HTS. Consequently, the relationship between pouring temperature and HTS is far from straightforward: a moderate superheat improves casting integrity by enhancing fluidity and feeding efficiency, whereas both excessively high and low pouring temperatures exacerbate HTS.

HTS generally decreases with increasing mold temperature, as shown in Fig. 3(b). Higher mold temperatures reduce the temperature gradient within the casting, which in turn lowers the accumulation of localized strain, a factor known to trigger hot tearing. During solidification, regions of concentrated thermal strain may develop due to uneven cooling; if such strain exceeds a critical threshold, cracks form. A higher initial mold temperature slows the solidification process, allowing the residual liquid sufficient time to accommodate accumulated strain and promote grain boundary bridging, thus enhancing hot tearing resistance[65, 67]. Moreover, elevated mold temperatures improve the efficiency of liquid feeding during solidification. Slower cooling rates at higher mold temperatures produce coarser and more continuous microstructures, with thicker residual liquid films that can more effectively fill developing cracks. This not only reduces stress concentration at grain boundaries but also raises the hot tearing initiation temperature, further facilitating the compensation for solidification shrinkage. Conversely, lower mold temperatures accelerate solidification, increasing solute segregation and localized strain. Faster cooling also enhances undercooling, thereby lowering the actual nucleation temperature of the primary phases and the eutectic reaction temperature, which aggravate HTS. In addition, accelerated solidification shifts the composition most susceptible to cracking toward higher solute contents[37]. At the end of solidification, alloy shrinkage induces substantial plastic deformation in the interdendritic liquid film at hot spot, which can lead to film rupture.

According to Lin et al.[54], the shrinkage strain (ε_b) can be given by:

$$\varepsilon_b = \frac{\alpha \Delta T L d}{l^2} \tag{4}$$

where α is the thermal expansion coefficient, ΔT denotes the solidification temperature range, L is the casting length, l is the hot joint length, and d is the grain diameter. This relation indicates that increasing the mold temperature leads to a larger grain size. Meanwhile, the hot joint length l is highly sensitive to mold temperature, and its square is inversely proportional to the solidification shrinkage strain. As a result, a higher initial mold temperature effectively alleviates shrinkage stress, reducing the HTS of the castings. Overall, elevating mold temperature promotes better strain accommodation, more effective interdendritic feeding, and improved grain coalescence, all of which collectively decrease the HTS.

The geometric characteristics of the castings and the deformability of the mold constitute critical extrinsic factors influencing hot tearing. The rigidity or compliance of the mold governs the degree to which the casting can accommodate thermal contraction during solidification. Rigid molds strongly constrain the solidifying alloy, leading to rapid accumulation of tensile stresses in semi-solid regions and promoting initiation of hot tearing. In contrast, molds with higher compliance can partially absorb shrinkage strains, mitigating local stress concentrations and reducing the likelihood of cracking[9]. Moreover, casting's geometry, including wall thickness, cross-sectional profile, and the presence of corners or abrupt changes, significantly affects the distribution of thermal stress and strain, with thicker sections or sharp corners being particularly prone to stress localization and crack formation[7]. The combined effect of mold deformability and casting geometry establishes the macroscopic mechanical boundary conditions during solidification, which are essential for accurately assessing HTS and guiding mold and casting design strategies in practice.

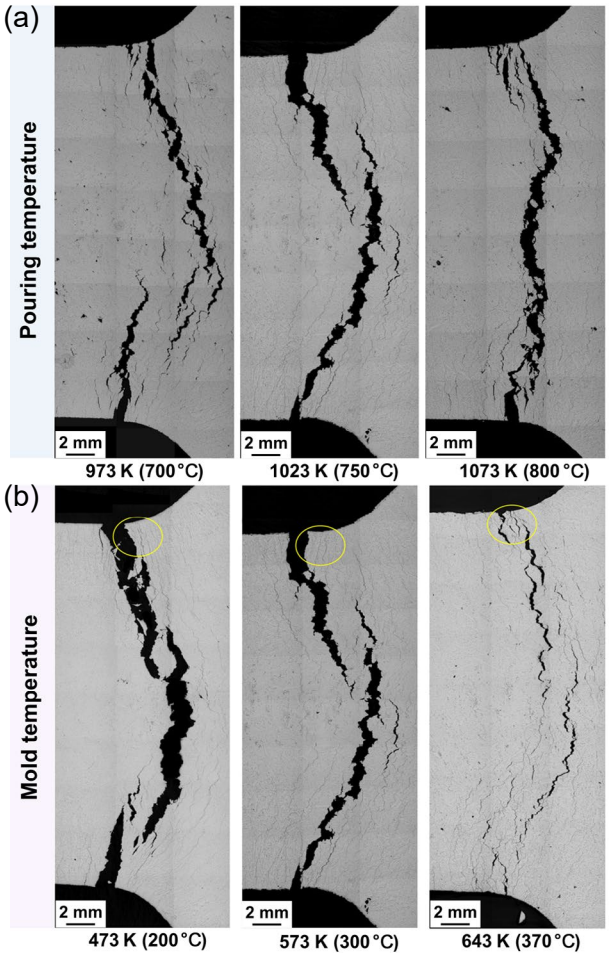

Fig. 3: Influence of casting parameters on HTS of an Al-Cu alloy (M206)[65]: (a) pouring temperature; (b) mold temperature

3.4 Inclusions

Inclusions can profoundly influence the HTS of cast Al alloys. Coniglio and Cross[68] experimentally demonstrated that during casting, folded oxide films formed on the melt surface may be entrained into the liquid metal upon pouring. Such non-metallic inclusions or liquid films serve as preferential sites for crack initiation. Nevertheless, compared with the extensive research on alloy composition and casting parameters, relatively little attention has been devoted to the role of inclusions in controlling HTS. This is partly because alloy composition and processing conditions are of more immediate industrial relevance, and partly because most mature commercial Al alloys can effectively suppress oxidation during melting through conventional degassing and refining procedures. However, our recent studies have revealed that inclusions play a dominant role in determining HTS in the Al-Li alloy system due to the extremely high chemical reactivity of the melt[69–73]. Experimental results showed that the HTS of Al-2Cu-*x*Li alloys exhibited two distinct peaks as a function of Li content, occurring at 1wt.% Li and 4wt.% Li, as shown in Fig. 4. The peak at 1wt.% Li can be attributed to the wide solidification temperature range, whereas the anomalous peak at 4wt.% Li cannot be explained by this factor as the solidification temperature range at this composition is relatively narrow[69].

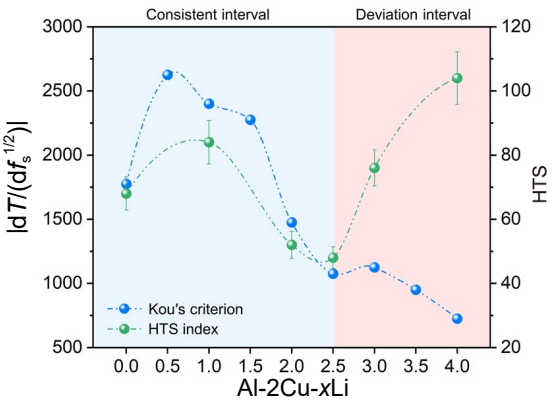

Fig. 4: Comparison plots of the experimental HTS index with Kou's criterion in Al-Cu-Li alloys[69]

After systematically excluding other potential causes, we identified that the severe HTS of Al-2Cu-4Li alloy originates from the presence of numerous micron-sized Li-rich inclusions, such as Li_2O, $LiAlO_2$, and Li_2CO_3, distributed within interdendritic regions [Figs. 5(a) and 5(b)]. Subsequent studies revealed that Li addition dramatically enhances the reactivity of the melt at elevated temperatures [Fig. 5(d)]. As a result, alloys with high Li contents, particularly near the solid solubility limit, readily react with O_2, CO_2, and H_2O during the final stages of solidification. The resulting oxidation products form spontaneously due to their highly negative Gibbs free energy change and high melting points. Moreover, the large discrepancy between the thermal expansion coefficient (27.8×10^{-6} K^{-1}) and elastic modulus (51.8 GPa) of the Al matrix versus the Li-rich inclusions (Table 1) reduces strain compatibility and induces stress localization within the mushy zone[74–80]. In addition to weakening interfacial bonding, the inclusions physically obstruct the narrow interdendritic channels, hindering residual liquid feeding. Importantly, these inclusions fail to contribute to grain refinement, contrary to some previous reports. Nanoparticles reported to promote grain refinement (e.g., TiC[57], Al_2O_3[58], MgO[81]) are deliberately introduced using controlled methods to achieve uniform distribution. In contrast, Li-rich inclusions arise spontaneously due to the high chemical reactivity of Li at elevated temperatures, segregate in interdendritic regions, and form non-uniform distributions.

Table 1: Physicochemical parameters of Li-rich oxidation products in Al-Li alloys[82-84]

Oxidation product	Reaction process	Free energy change (kJ)	Melting point (°C)	Thermal expansion coefficient (10^{-6} K^{-1})	Elastic modulus (GPa)
Li_2O	$4Li + O_2 \rightarrow 2Li_2O$	−988.4	1,567	35.2	134.7
Li_2CO_3	$1.33Li + CO_2 \rightarrow 0.66Li_2CO_3 + 0.33C$	−263.2	720	38.9	116.5
$LiAlO_2$	$Li + Al + O_2 \rightarrow LiAlO_2$	−1,018.4	1,900	12.2	204.2

Computational fluid dynamics (CFD) simulations of interdendritic pressure drops further confirm that the presence of Li-rich inclusions increases the pressure drop by approximately an order of magnitude compared to a clean melt[72]. This insufficient pressure prevents the residual liquid from effectively compensating for shrinkage cavities, thereby promoting microcrack initiation and propagation, thus ultimately leading to irreversible cracking [Fig. 5(c)]. Beyond restricting interdendritic flow and reducing melt permeability, Puncreobutr et al.[85] suggested that such inclusions may also act as diffusion barriers, impeding hydrogen transport in the interdendritic liquid. This can locally induce hydrogen supersaturation, triggering pore nucleation within confined regions. Although vacuum melting can partially reduce the HTS of Al-Li alloys by suppressing melt oxidation, this approach is challenging to scale up for industrial production. Therefore, in producing Li-containing Al alloys, especially those with high Li contents, the fundamental challenge lies in optimizing melting practices to improve melt quality and minimize oxidation. Addressing this challenge is essential to reducing HTS and enabling their broader industrial application.

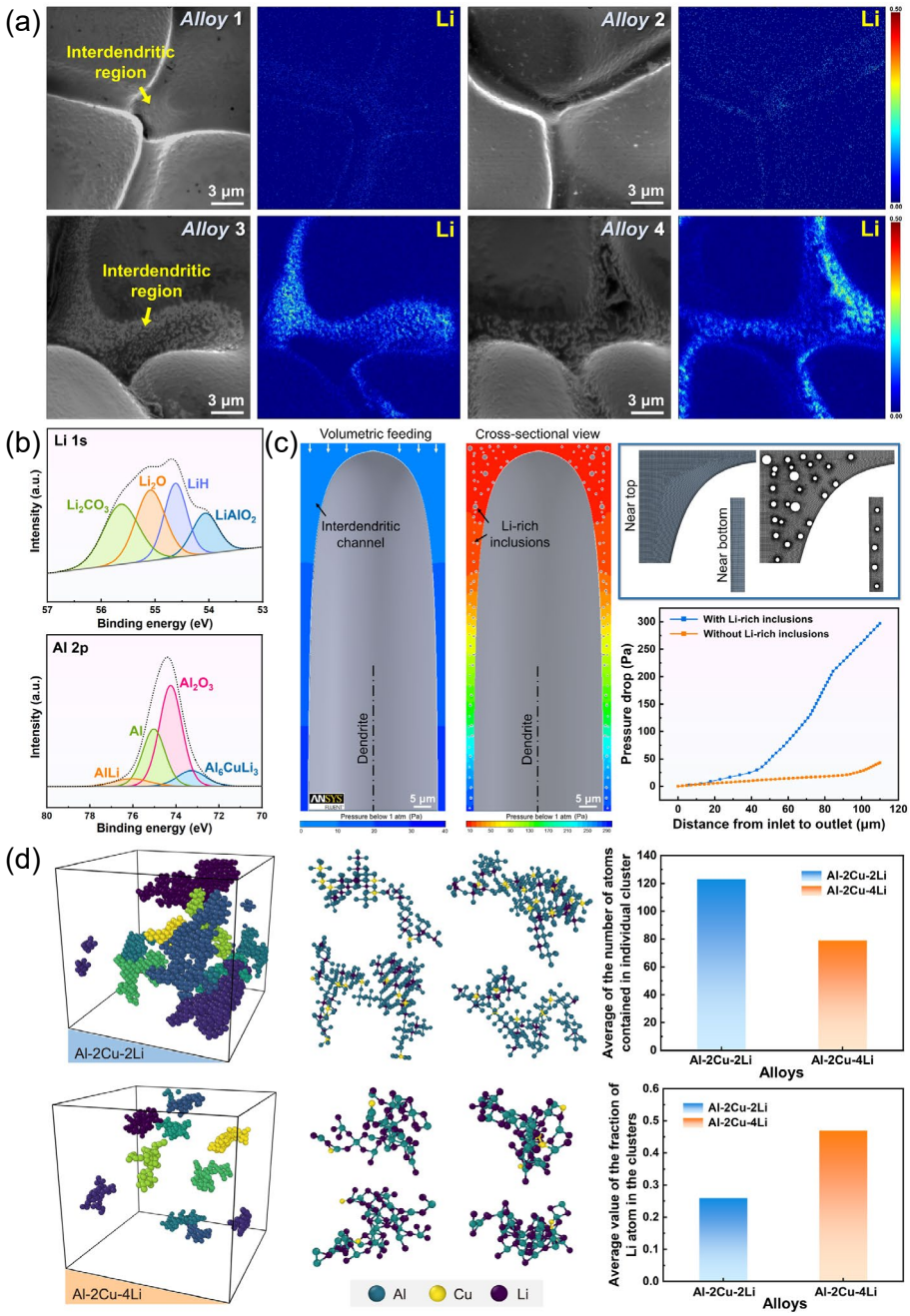

Fig. 5: Influence of interdendritic Li-rich inclusions on HTS in Al-Li alloys: (a) time-of-flight secondary ion mass spectrometry (ToF-SIMS) images of interdendritic regions showing the distribution of Li-rich inclusions[72]; (b) X-ray photoelectron spectroscopy (XPS) spectra[72]; (c) pressure distribution in interdendritic regions of alloys with and without Li-rich inclusions[72]; (d) simulated cluster morphology and key features of clusters[73]

4 Research methods evaluating hot tearing

4.1 Simple evaluation

The most straightforward methods for evaluating hot tearing rely on post-solidification inspection, which can be broadly categorized into macroscopic and microscopic approaches. At the macroscopic level, techniques such as dye or wax penetrant testing, ring mold testing [Fig. 6(a)][91], and constrained rod casting (CRC) testing [Figs. 6(b) and (c)][92-93] are commonly used to detect surface cracks[86-90]. These methods are favored for their simplicity, low cost, and rapid identification of both the presence and extent of hot tears. At the microscopic level, metallographic techniques including optical microscopy (OM) and scanning electron microscopy (SEM) enable a detailed characterization of crack initiation sites, propagation paths, and interactions with dendrites, eutectic phases, or inclusions. While these approaches provide valuable insights into the severity and morphology of hot tears, their quantitative accuracy is often limited, making reliable assessment of crack volume or severity challenging. Moreover, they are inherently post-mortem analyses, revealing only the final state of cracking

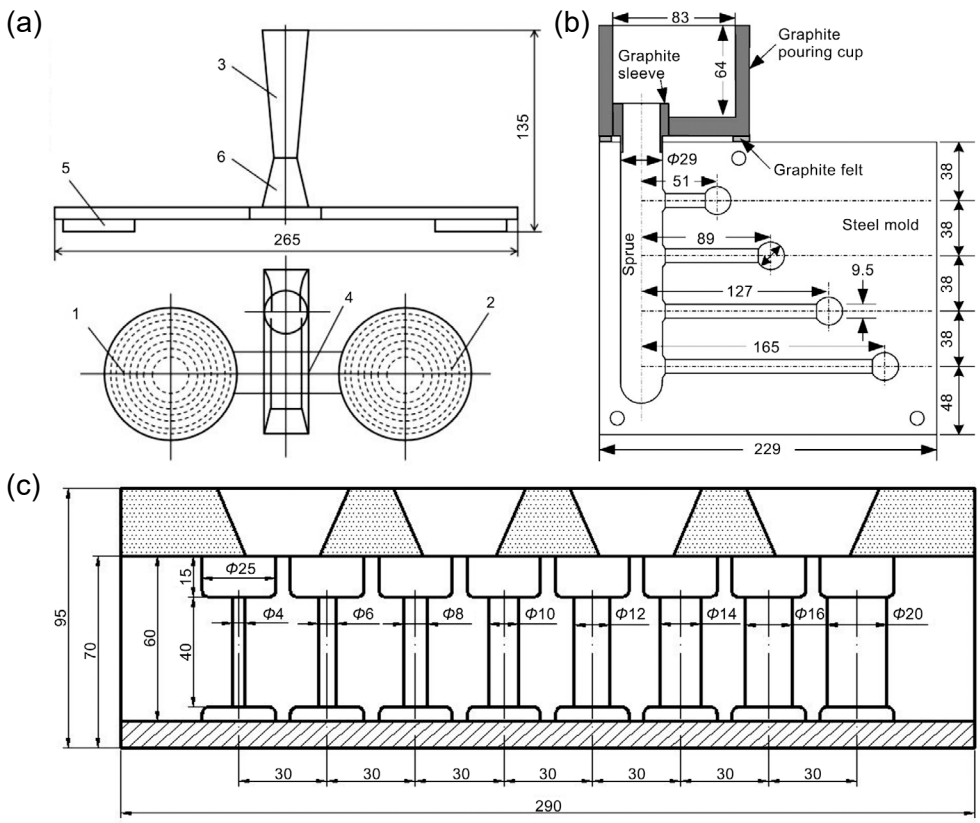

Fig. 6: Representative apparatus for simple hot tearing evaluation: (a) ring mold[91]; (b) CRC mold of critical length[92]; (c) CRC mold of critical diameter[93] (Unit: mm)

after solidification, with minimal information on the dynamic nucleation and growth processes that govern hot tearing during the semi-solid stage. Therefore, simple evaluation methods are insufficient for researchers aiming to elucidate the underlying mechanisms of hot tearing. Numerous studies have provided comprehensive reviews of their application scenarios, operating procedures, and experimental outcomes, and interested readers are referred to those works for further details[6, 7, 9].

4.2 Physical parameter-based evaluation

Physical parameter-based approaches for evaluating hot tearing can be broadly classified into three types: apparatus that records load and temperature, apparatus that records load and displacement, and semi-solid tensile testing that provides stress-strain data. The first two types are largely derived from the classical CRC setup, with additional sensors and data acquisition systems integrated to capture the thermal and mechanical responses during solidification, as shown in Fig. 7. For instance, Cao et al.[94] modified the traditional four-channel CRC mold by adding an auxiliary channel at the bottom and equipping it with temperature-load sensors, enabling simultaneous monitoring of contraction force and temperature [Fig. 7(a)]. The magnitude of the load drop reflects the HTS, while the corresponding temperature identifies the onset of cracking, from which the solid fraction at fracture can be inferred. Such data are crucial for elucidating the conditions under which cracks initiate and propagate in the mushy state. To overcome the operational complexity and bulkiness of conventional CRC setup, as well as the known influence of specimen length on HTS measurements, a simplified T-shaped CRC mold was subsequently developed[21, 88, 95–97] [Fig. 7(b)][95]. This design eliminates the length effect and facilitates more straightforward and reproducible testing. More recently, Su et al.[98, 99] proposed a multi-channel "cross-type" experimental device capable of simultaneously measuring contraction force and temperature evolution, thereby enabling a systematic investigation of the influence of wall thickness on hot tearing susceptibility [Fig. 7(c)][98].

Another CRC modification involves the integration of load-displacement sensors, allowing simultaneous monitoring of contraction force and rod displacement during solidification[100]. The underlying principle is that the measured displacement correlates with the HTS of the alloy. In tear-free alloys, the displacement detected prior to the non-equilibrium eutectic temperature is minimal, indicating stable contraction behavior. In contrast, alloys exhibiting severe hot tearing display much larger displacements, reflecting pronounced deformation associated with crack initiation and propagation. In addition, semi-solid tensile testing provides another robust approach to evaluate HTS by directly measuring failure strength and elongation in the mushy state[101–103]. This testing can be conducted either by reheating a solid sample to a temperature slightly above the solidus (i.e., remelting) or by cooling a liquid alloy to a temperature slightly below the liquidus (i.e., solidification). These differing thermal histories result in distinct semi-solid microstructures, which in turn influence the mechanical response recorded during testing.

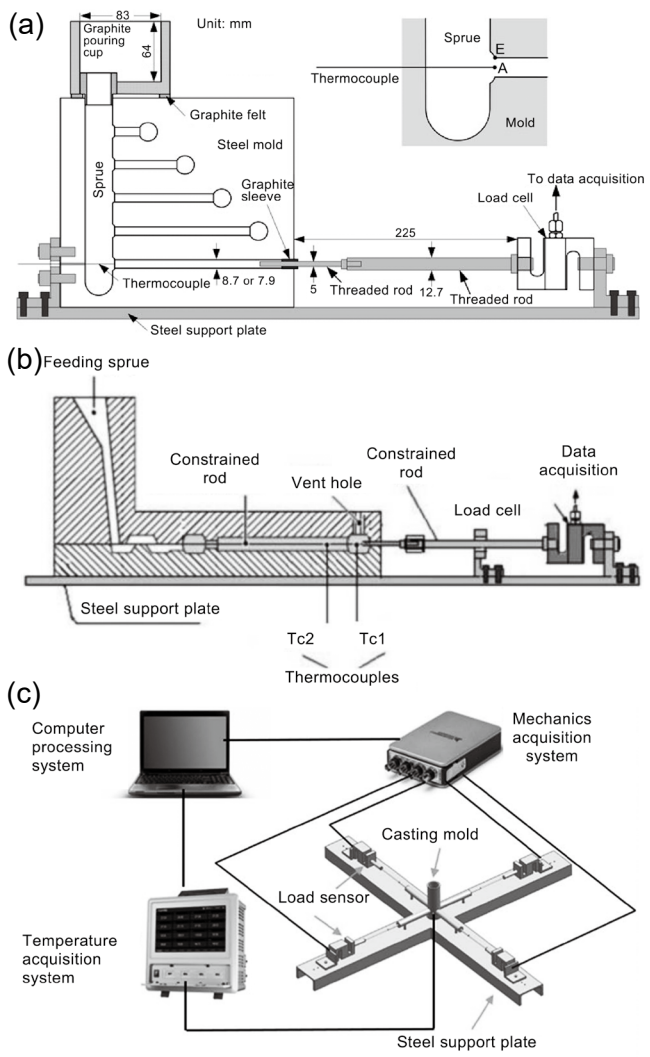

Fig. 7: Apparatus equipped with temperature-load recording system: (a) original CRC mold[94]; (b) T-shaped mold[95]; (c) multi-channel "cross-type" mold[98]

The principles, methodologies, and representative findings of semi-solid tensile testing have been thoroughly reviewed by Eskin[6] and Li[7]; interested readers are referred to these works for further details. These progressively refined apparatuses underscore the value of physical parameter-based evaluation in providing quantitative and mechanistic insights into hot tearing phenomena, offering a more comprehensive perspective than simple post-mortem observations. Nevertheless, these methods remain unable to capture the initiation and propagation of hot tears directly and in real time.

4.3 In situ observation

Previous investigations of hot tearing in Al alloys have largely relied on post-mortem analyses. While informative, such approaches cannot capture the real-time evolution of microstructure and defect formation during solidification, including the nucleation and propagation of pores and cracks. With recent advances in characterization techniques, in situ observation during casting and solidification processes has become feasible. Davidson et al.[104] employed mirror-reflection video imaging to study hot tearing in Al-Cu alloys, enabling direct visualization of crack initiation and propagation. Haaften et al.[105] performed in situ heating and tensile tests on AA5182 alloys within a SEM, capturing the separation of liquid films along grain boundaries and revealing the microscopic mechanisms underlying semi-solid deformation and crack development. However, these techniques are primarily limited to surface observations and cannot provide internal three-dimensional (3D) images, hindering the full visualization of the spatial distribution and 3D evolution of hot cracks.

Neutron diffraction offers a powerful means of real-time monitoring of hot tearing evolution within alloys. Its primary advantage lies in the exceptionally high penetration depth and stability of neutrons, which allows in-situ observation of large bulk castings. D'Elia et al.[106, 107] systematically investigated the hot tearing mechanisms of B206 Al alloy using neutron diffraction, focusing on the effects of mold temperature and Ti additions on HTS. Their findings revealed the evolution of the Al_2Cu phase during solidification as well as the strain distribution within the mushy zone skeleton, providing critical experimental evidence for a deeper understanding of hot tearing formation mechanisms. Nevertheless, neutron diffraction has limitations: access to neutron sources is highly restricted and costly, the detection efficiency is relatively low, and its spatial resolution (hundreds of microns to millimeters) makes it difficult to capture the very early stages of microcrack initiation and propagation.

Synchrotron X-ray imaging represents an advanced technique capable of real-time measurement of rapid transient phenomena, making it particularly suitable for capturing solidification kinetics and defect evolution. Owing to the high penetration power of X-rays in dense, optically opaque metallic materials combined with their high spatial and temporal resolution [Fig. 8(a)][114], this technique has been widely employed in studies of casting, welding, and additive manufacturing[108-113]. It enables direct visualization of interdendritic liquid feeding, strain localization, and micro-neck formation during semi-solid deformation [Fig. 8(b)][114]. Moreover, it allows quantification of hot tear initiation and propagation and elucidates the influence of microstructural features, such as secondary phases or Fe-rich intermetallic compounds, on interdendritic flow, crack distribution, and coalescence events, thereby clarifying the formation of the most severe and damaging cracks [Fig. 8(c)][115]. For instance, in situ observation of hydrogen microporosity in Al-Li alloys facilitates quantification of nucleation and growth kinetics of pores, as well as their final size, number, and irregularity, highlighting the effects of Li concentration[116]. Overall, synchrotron X-ray imaging not only provides real-time visualization of semi-solid and solidification processes but also delivers quantitative data on liquid flow, strain distribution, and microstructural evolution, offering critical experimental evidence for the development and validation of hot tearing and microporosity models.

With the advent of advanced synchrotron X-ray computed tomography (XCT), it has become possible to capture the 3D evolution of hot tearing in Al alloys with unprecedented

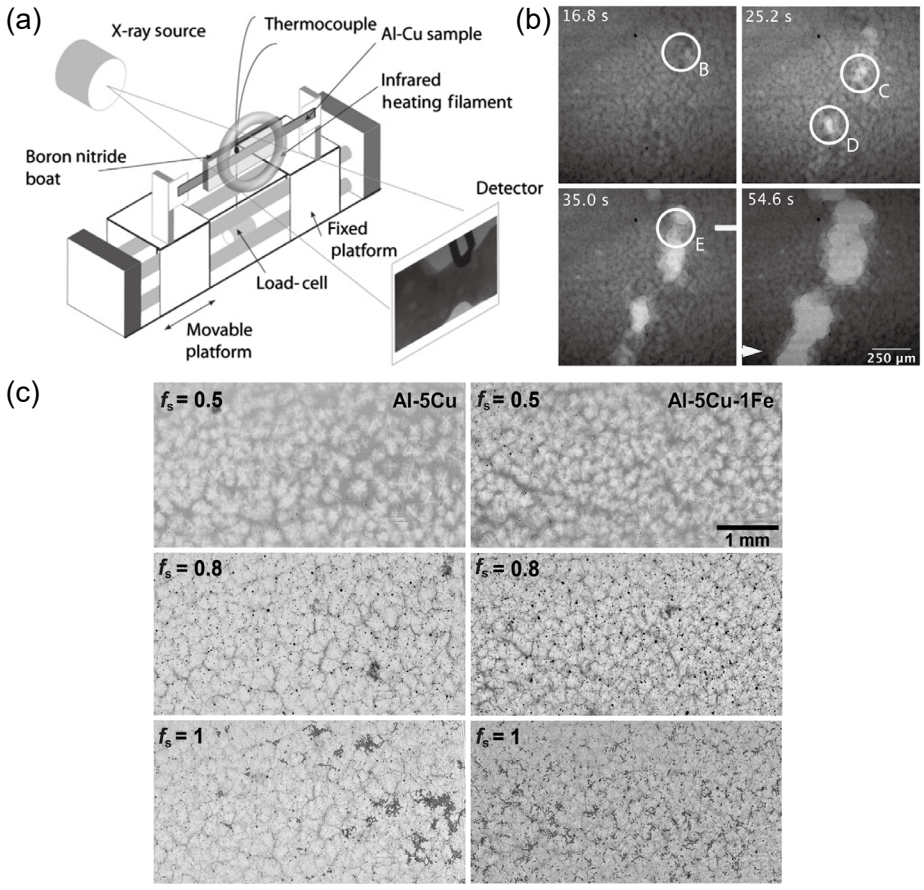

Fig. 8: Application of synchrotron X-ray in the study of hot tearing in cast Al alloys: (a) schematic diagram of in-situ observation via synchrotron X-ray imaging[114]; (b) evolution of strain localization and void coalescence during isothermal tensile deformation of semi-solid Al-12wt.% Cu at 580 °C[114]; (c) radiographs of Al-5Cu and Al-5Cu-1Fe alloys solidified at 1 °C·s^{-1}, in which f_s denotes the solid fraction[115]

spatial and temporal resolution. These techniques not only enable quantification of damage accumulation and porosity development during semi-solid deformation, but also provide unique insights into the role of alloy composition and intermetallic phases[117-119]. For instance, synchrotron XCT of semi-solid Al-Cu alloy under tensile loading has revealed that hot tear formation proceeds through sequential void nucleation, growth, and coalescence, with internal voids initiating at high-triaxiality regions and propagating outward, ultimately leading to failure due to insufficient liquid feeding [Fig. 9(a)][120]. Operando tomography has further shown that semi-solid deformation is highly heterogeneous, often accompanied by localized liquid accumulation at grain boundaries, followed by micropore nucleation once liquid feeding becomes inadequate[121]. Moreover, Fe-rich intermetallics have been demonstrated to exacerbate HTS by obstructing interdendritic channels, promoting pore growth along their surfaces due to interfacial energy differences, and ultimately inducing a transition from ductile-like to brittle-like fracture modes [Fig. 9(b)][85]. Beyond simple defect characterization, synchrotron imaging combined with advanced segmentation and modeling has elucidated the complex 3D network structures of Fe-containing phases, their morphological evolution, and their influence on shrinkage feeding and crack propagation[122]. In particular, the dynamic nucleation and growth of convoluted Fe-rich phases have been directly observed, and external fields such as ultrasound have been shown to effectively refine both dendritic and intermetallic morphologies, thereby mitigating solidification defects [Fig. 9(c)][121]. Taken together, these findings highlight the transformative potential of in situ synchrotron tomography in uncovering the interplay among liquid feeding, pore evolution, and intermetallic morphologies during hot tearing. Looking forward, coupling such real-time imaging with precisely controlled hot tearing test rigs would allow simultaneous correlation of microstructural observations with quantitative load, displacement, and temperature data.

4.4 Numerical simulation

With the rapid advancement of computer technologies, numerical simulation has found widespread applications in industrial production. Its primary advantage lies in substantially reducing the time and resource requirements for new product development, thereby markedly shortening the design cycle. In recent years, as mathematical and theoretical models have been continually refined, an increasing number of theoretical studies have been effectively implemented through numerical simulations, with their accuracy and applicability rigorously validated across diverse fields. Thermodynamic calculation software based on phase diagrams, such as Pandat, Thermo-Calc,

and JMatPro, can not only predict phase constitutions and solidification paths for casting Al alloys with varying compositions, but also estimate relevant thermophysical properties, including volumetric shrinkage, thermal expansion coefficients, and viscosity[123–125]. These predictions provide reliable input for subsequent casting simulations of Al alloys, process optimization, and parameterization of various hot tearing criteria.

Finite element analysis (FEA) offers an effective framework to capture coupled thermo-mechanical-fluid interactions during alloy solidification, overcoming the spatiotemporal limitations inherent in in-situ experimental observations. Within this framework, commercial packages such as ProCAST, Anycasting, Abaqus, and ANSYS Fluent have been extensively applied to simulate temperature evolution, stress-strain development, and liquid feeding behavior, and to predict HTS when integrated with appropriate criteria[126–130]. For example, the hot tearing indicator (HTI) embedded in ProCAST has proven effective in evaluating HTS under industrial casting conditions [Fig. 10(a)][131]. At the microscale, direct finite element models based on modified Voronoi tessellations have been employed to capture the deformation behavior of semi-solid alloys, linking grain size, porosity, and strain localization to macroscopic constitutive responses[132]. Building upon this, coupled finite element approaches explicitly incorporate intergranular liquid films, enabling prediction of strain localization during solidification and advancing toward quantitative hot tearing prediction [Fig. 10(b)][133]. Complementary simulations, validated by in situ X-ray radiography, further elucidate the local contraction and dilation of grain assemblies, heterogeneous strain fields, and fluctuations in liquid pressure. These insights support the perspective that semi-solid alloys can be effectively described within the conceptual framework of critical state soil mechanics[134]. In parallel, FEA-based thermal stress analyses highlight the influence of grain size on creep parameters, demonstrating that grain refinement homogenizes strain distribution and reduces peak strain, thereby mitigating HTS[135]. Concurrently, new hot tearing criteria have been

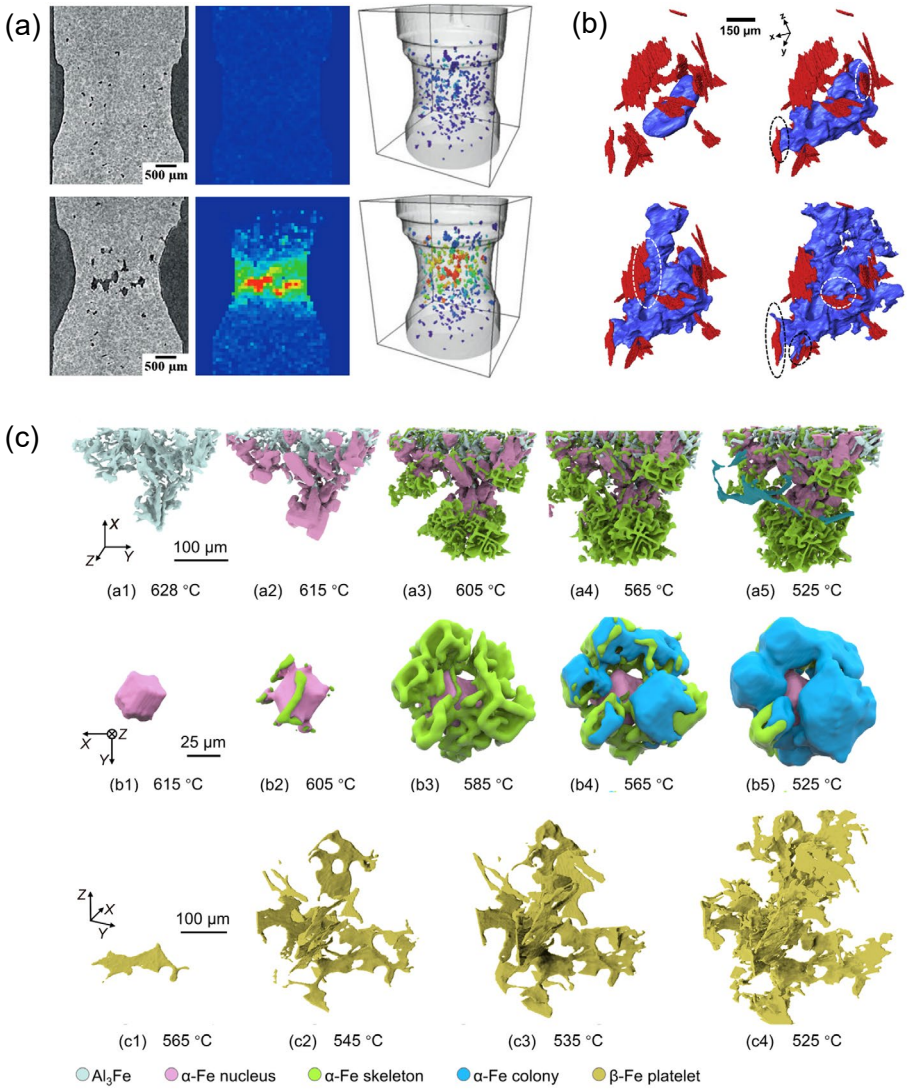

Fig. 9: Application of synchrotron XCT in the study of hot tearing in cast Al alloys: (a) 3D rendering of pore evolution (blue) in the presence of intermetallic in A319 alloy[85]; (b) 3D images obtained by semi-solid tensile testing of an Al-15Cu alloy[120]; (c) 3D morphology evolution of three different Fe-containing phases in a typical recycled Al-5Cu-1.5Fe-1Si alloy[121]

proposed to extend the predictive capability of FEA. Sistaninia et al.[136] developed an advanced hot tearing criterion within the Abaqus platform, while Liu et al.[137] implemented a fluid-structure interaction-based criterion in ANSYS Fluent. These approaches will be discussed in detail in Section 5. It should be emphasized, however, that the application of FEA to hot tearing prediction remains largely confined to alloy systems that are well characterized and supported by comprehensive thermo-mechanical property databases, limiting its current generalizability to novel alloy design.

Molecular dynamics (MD) simulations have proven particularly effective in characterizing the structural and dynamical properties of metallic melts, thereby offering unique insights into hot tearing phenomena at the atomic scale. A key contribution of MD lies in its ability to predict transport properties, such as diffusion coefficients and viscosity, which govern liquid feeding and crack healing. For instance, alloying-induced modifications in the liquid structure can significantly influence atomic mobility: Zr additions to Al markedly suppress Al self-diffusion due to the formation of strongly correlated clusters[138], whereas Cu dissolution in liquid Al enhances tracer diffusivity and modifies viscosity via the emergence of locally ordered motifs[139]. These findings emphasize that short-range structural ordering, beyond mere chemical composition effects, critically dictates liquid fragility, atomic transport, and ultimately feeding capacity during solidification. Extending this framework, the integration of MD with experimental observations has further clarified the role of liquid films in crack initiation by Su and Zhang[140, 142–145]. It has been demonstrated that variations in liquid fraction, viscosity, and atomic activity of residual liquid channels at the end of solidification directly affect the critical stress required for crack formation. Highly fluid films promote defect healing and mitigate the severity of hot tearing. Collectively, these results underscore the unique capability of MD to elucidate the atomistic origin of diffusion, viscosity, and interfacial phenomena that govern HTS. Nevertheless, the intrinsic limitations of MD in accessible spatial and temporal scales preclude direct predictions of macroscopic crack evolution, necessitating its coupling with mesoscopic or continuum-scale models for comprehensive and predictive simulations of hot tearing.

Phase-field simulations represent a state-of-the-art tool for coupling phase, temperature, and solute fields, enabling continuous tracking of dendrite growth, grain impingement, solute segregation, and liquid channel evolution during solidification. These capabilities allow phase-field models to directly link microstructural evolution with the underlying mechanisms of hot tearing[146, 147]. Simulation studies indicate that the morphological evolution and solute segregation behavior of liquid channels exert a strong influence on HTS [Fig. 11(a)][44]. In Al-Cu alloys, limited back-diffusion and incomplete coalescence of liquid channels promote droplet formation, while eutectic solidification near channel roots reduces cracking. In contrast, Al-Mg alloys, despite possessing a wide freezing range, exhibit lower HTS due to enhanced dendrite coalescence facilitated by Mg back-diffusion[39].

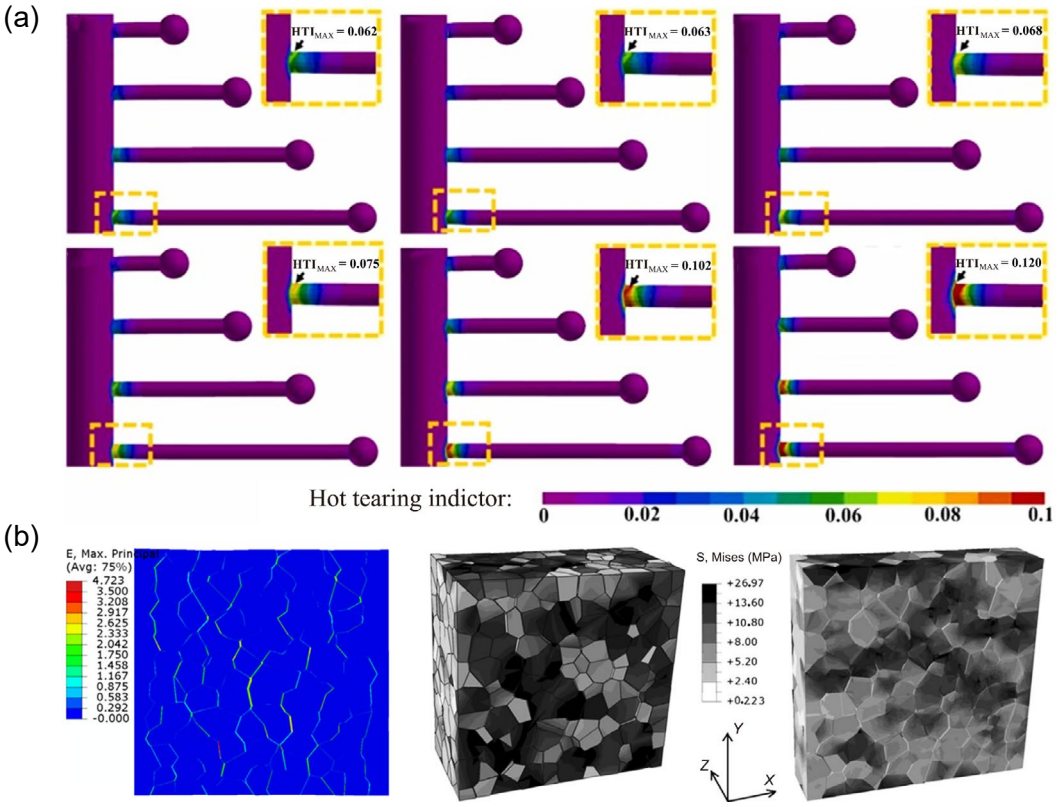

Fig. 10: Application of FEA in the study of hot tearing in cast Al alloys: (a) simulation result showing the HTI of Al-5.4Mg-2Si alloys with various Cu contents[131]; (b) strain localization and von Mises stress of Al-Cu alloys under tensile deformation at f_s=0.98[133]

Parametric analyses further show that increasing solid-state diffusivity or partition coefficients can flatten the solid fraction-temperature relationship, suppress solute segregation, and thereby mitigate cracking [Fig. 11(b)][40]. Recent simulations also highlight the critical role of solidification shrinkage, showing that density changes during the liquid-to-solid transformation constrict and elongate liquid channels, elevate pressure drops at their roots, and consequently exacerbate HTS[148]. Integrated phase-field-computational fluid dynamics (PF-CFD) approaches extend predictive capability by quantifying interdendritic fluid flow and pressure drops[149]. Such models reveal that grain orientation, equiaxed grain size, and columnar-to-equiaxed transition significantly alter feeding conditions and HTS in Al-Li alloys, surpassing the predictive resolution of conventional analytical models [Fig. 11(c)][149]. Overall, phase-field simulations offer powerful means to elucidate liquid channel evolution and dendrite coalescence, providing mechanistic insight into hot tearing. Yet challenges remain in computational cost and experimental validation. Future efforts that integrate phase-field simulations with multi-scale modeling and in situ characterization will be essential to establish a reliable predictive framework.

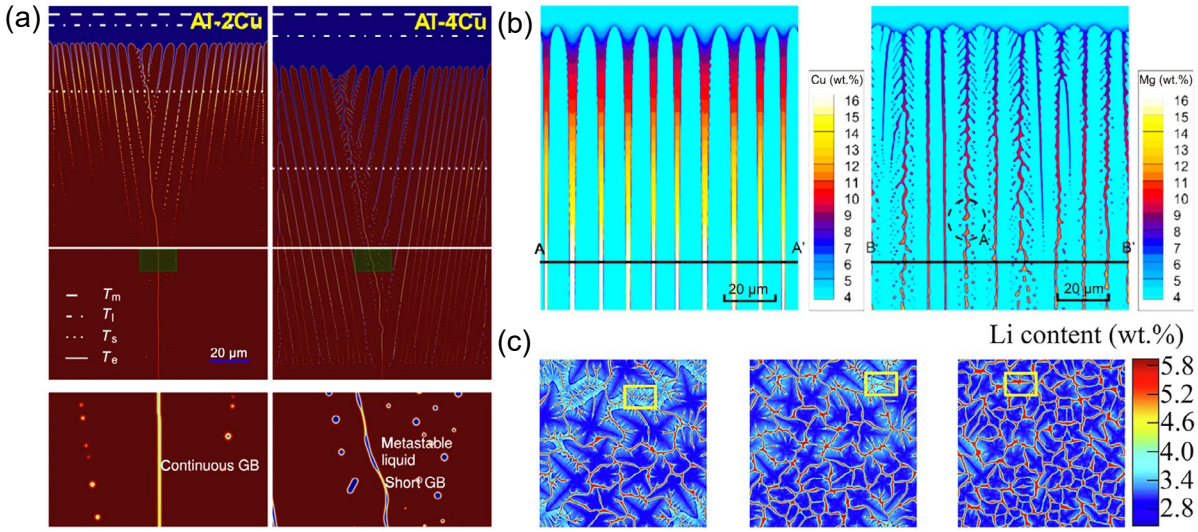

Fig. 11: Application of phase-field simulations in the study of hot tearing in cast Al alloys: (a) liquid channels during bi-crystal columnar growth of Al-Cu alloys[44]; (b) solute distribution within liquid channels during columnar growth of Al-Cu and Al-Mg alloys[40]; (c) liquid channel concentration in equiaxed crystals with different grain sizes at a solid fraction of 0.9[149]

5 Hot tearing criteria

The prediction of HTS has long been a central challenge in alloy casting[150-153]. In industrial practice, HTS reduction is often achieved through repeated trial-and-error adjustments of alloy compositions and process parameters, which is both costly and time-consuming. Hence, the development of accurate and reliable predictive criteria for HTS is of great practical significance. Since the 1950s, numerous criteria have been proposed based on different theories and assumptions, which can be broadly classified in two ways[154-157]. The first distinction is between analytical criteria and numerical simulation approaches. Analytical criteria are typically expressed in concise algebraic forms with clear physical interpretations, providing a single scalar index or threshold for evaluating HTS. This enables rapid, quantitative assessment, making these criteria particularly attractive for early-stage alloy screening or comparative studies. Their primary advantage lies in simplicity and computational efficiency[158-161]. By contrast, numerical simulation approaches are established on coupled governing equations describing heat transfer, fluid flow, solidification, and stress/strain evolution. These methods aim to capture the spatiotemporal development of hot tearing during solidification in a physically representative manner. However, they require extensive input data, including thermophysical properties, initial and boundary conditions, mesh discretization, and time steps, and the numerical solution of partial differential equations often demands computational times ranging from several hours to days[162-165].

The second classification distinguishes mechanical-based, non-mechanical-based, and comprehensive criteria[166-170]. Mechanical-based criteria mainly focus on the response of the semi-solid skeleton, with stress, strain, and strain rate as the dominant variables. Non-mechanical-based criteria emphasize thermal and metallurgical factors, such as the vulnerable temperature ranges, phase diagram characteristics, and casting process parameters. Comprehensive criteria attempt to integrate both mechanical and non-mechanical aspects into a unified framework. Although comprehensive criteria often yield improved predictive accuracy, they inevitably incur more mathematically complex and data-demanding. To date, numerous reviews have summarized the mechanisms and applications of various hot tearing criteria developed for casting alloys. Given this extensive literature, the present paper does not intend to cover all existing models exhaustively. Instead, attention is focused on a selection of recently

proposed promising approaches. Readers interested in other criteria or in-depth analyses of specific models are referred to several authoritative publications[6, 7, 9].

5.1 Steady-state axisymmetric numerical model and axisymmetric analytical model

In 2023, Liu et al.[137] developed a steady-state axisymmetric numerical model based on CFD to predict the HTS of alloys. The model determines the pressure distribution and velocity field of the liquid within interdendritic channels through numerical simulations [Fig. 12(a)], with the maximum pressure drop as an indicator of HTS. Unlike the RDG model, this approach does not treat the mushy zone as a porous medium. Instead, it directly computes the dendrite shape in the mushy zone from the temperature (T) vs. f_s relationship and solves the Navier-Stokes equations, while incorporating the influence of back diffusion. As a result, the model provides a more realistic and accurate representation of liquid flow within dendrites. It has been successfully applied to predict the HTS of binary Al-Cu and Al-Mg alloys during welding. Building upon this CFD model, Liu proposed an axisymmetric analytical model in 2024[171]. In this new model, the pressure drop (Δp) is given by:

$$\begin{aligned}\Delta p &= p\big|_{Z=L} - p\big|_{Z=0} \\ &= \frac{16\pi}{\sqrt{3}(\lambda_1)^2 G^2}\int_{T_f}^{T_t}\frac{2\mu\int_{T_f}^{T}\dot{\varepsilon}\,\mathrm{d}T}{-2\ln(f_S)-3+4f_S-f_S^2}\mathrm{d}T \\ &+ \frac{16\pi V\beta}{\sqrt{3}(\lambda_1)^2 G}\int_{T_f}^{T_t}\frac{\mu(1-f_S)}{-2\ln(f_S)-3+4f_S-f_S^2}\mathrm{d}T\end{aligned} \tag{5}$$

where L is the position of the dendrite tips along the Z-axis, while 0 denotes the position of the dendrite roots. λ_1 represents the primary dendrite arm spacing, G is the temperature gradient in the Z-direction, μ is the viscosity, β is the solidification shrinkage, V is the growth rate, $\dot{\varepsilon}$ is the lateral strain rate, and T_f and T_t denote the start and end temperatures of solidification, respectively. Although both the CFD and analytical models exhibit similar reliability in predicting the HTS of Al-Cu alloys [Fig. 12(b)][171], the analytical model offers significantly higher computationally efficiency, requiring only a few seconds compared to several hours for CFD simulations. Collectively, these two models proposed by Liu et al. represent a powerful extension of the RDG model, offering enhanced physical realism in describing interdendritic liquid feeding while also improving computational efficiency. Nevertheless, several limitations remain. First, dendrite growth is simplified as axisymmetric, and the effect of grain boundary misorientation is neglected, potentially overlooking complex growth phenomena in real alloys. Second, the models emphasize mainly on pressure drop and liquid flow, failing to fully capture the multi-stage nature of hot tearing, particularly the role of grain boundary bridging. Third, further modifications are required to adapt the framework to equiaxed grain structures, thereby accounting for the influence of diverse alloy microstructures on HTS.

5.2 Criterion based on characteristics of liquid film and microstructure

In 2023, Su et al.[172] proposed a hot tearing criterion that integrates the characteristics of solidification liquid films and microstructure, building upon the foundations of both the RDG and Kou's criteria. This criterion integrates mechanical and non-mechanical factors during solidification, incorporating the shrinkage volume of the solid-liquid two-phase in the mushy zone, the flow behavior of liquid film, and the influence of microstructure on feeding behavior. It also incorporates additional factors such as alloy composition, microstructure, mold design, and process conditions, all of which significantly affect the initiation of hot tearing. The principal advantage of this approach over the original RDG and Kou's criteria is its ability to quantitatively predict whether hot cracks will actually occur during solidification, rather than simply providing a relative index of HTS. According to Su, the initiation and severity of hot tearing are closely related to three competing volumetric contributions: the change in solid grain volume due to thermal shrinkage (V_S); the change in the liquid film volume between adjacent solid grains due to linear shrinkage (V_L); and the difference between the sum of these two and the feeding volume of the liquid film ($V_{feeding}$) between the adjacent grains, as shown in Fig. 13(a)[172]. Specifically, if the sum of V_S and V_L minus $V_{feeding}$ is positive, hot tearing will occur; otherwise, it will not. Based on this principle, the hot tearing criterion is expressed as:

$$\begin{cases}\dfrac{4}{3}\pi a_0 b_0^2\left\{1-\left[(1-\alpha)\Delta T\right]^3\right\}+\left(4a_0b_0L_0-\dfrac{4}{3}\pi a_0b_0^2\right)-\left(4a_0c_0L_0-\dfrac{4}{3}\pi a_1b_1^2\right) \\ \qquad > -n\dfrac{\pi r^{*4}}{8\eta l^*}\Delta P^* t \qquad \text{hot cracks will occur} \\ \dfrac{4}{3}\pi a_0 b_0^2\left\{1-\left[(1-\alpha)\Delta T\right]^3\right\}+\left(4a_0b_0L_0-\dfrac{4}{3}\pi a_0b_0^2\right)-\left(4a_0c_0L_0-\dfrac{4}{3}\pi a_1b_1^2\right) \\ \qquad \le -n\dfrac{\pi r^{*4}}{8\eta l^*}\Delta P^* t \qquad \text{hot cracks will not occur}\end{cases} \tag{6}$$

where α is the linear expansion coefficient, ΔT is the temperature gradient variates, n is the number of feeding channels, r^* is the radius of the feeding channel, l^* is the length of the feeding channel, η is the dynamic viscosity, ΔP^* is the pressure difference between the outlet and the inlet of the feeding channel, t *is* the liquid film flow feeding time, and a_0, b_0, L_0, a_1, b_1 are parameters related to grain geometry, respectively [Fig. 13(b)]. These parameters, including η, ΔP^*, l^*, r^*, and n, are directly linked to the liquid film characteristics and microstructure, which are further controlled by temperature, alloy composition, grain size, and other microstructural factors. This criterion has been successfully

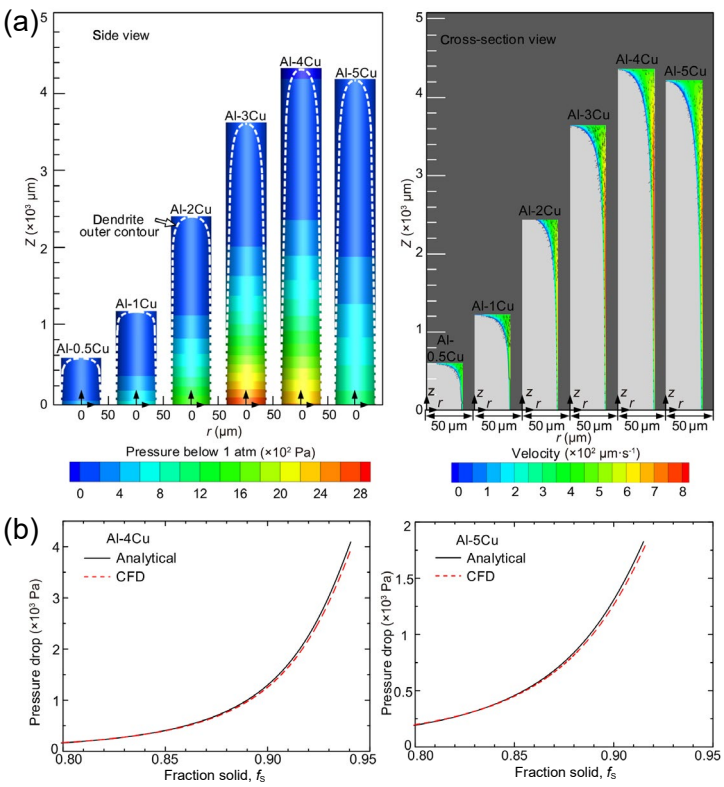

Fig. 12: Liu's models for predicting HTS in Al alloys: (a) pressure drop in liquid channel and velocity distribution[137]; (b) comparison of pressure drop calculated by analytical model and CFD model[171]

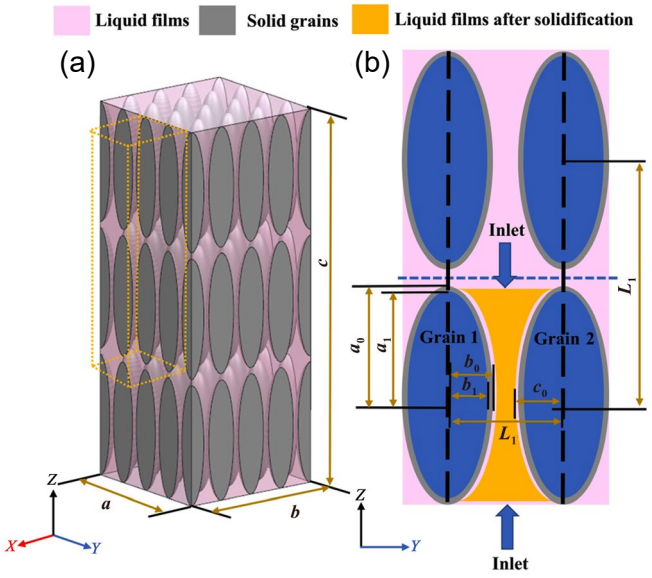

Fig. 13: Schematic diagram of Su's model[172]: (a) macroscopic scale; (b) microscopic scale

applied to predict the HTS of Al-4Cu alloys, with predictions showing good agreement with experimental data, thus validating its reliability[172]. However, this criterion simplifies the physical assumptions by concentrating primarily on shrinkage and liquid film flow while neglecting other thermodynamic and mechanical complexities, potentially leading to predictive inaccuracies in more complex scenarios. Moreover, its strong dependence on grain morphological parameters limits its adaptability across different alloy systems, particularly when grain shapes are influenced by factors like cooling rates.

5.3 Model based on solid bridge fracture

In 2024, Liu et al.[173] proposed a novel model based on solid bridge fracture to predict solidification cracking in alloys, as shown in Fig. 14. Unlike conventional models that rely primarily on liquid feeding, this model introduces a crack-like structure to directly evaluate the thermal stress at the dendrite roots. The occurrence of cracks depends on the competition between thermal stress accumulation at the dendrite roots and the development of solid bridge strength, while also accounting for the influence of grain morphology and size on stress accumulation. This model is based on the following considerations: (a) The necessary condition for crack-free solidification is that during the bridging stage ($f_{brid} \le f_s < 1$), the rapidly developing strength of the solid bridges must be sufficient to counteract the accumulated thermal stresses within the bridges; (b) Stress singularities do not arise at dendrite roots, meaning that initial fracture does not occur and solid bridges can form progressively; (c) Liquid channels along grain boundaries play a dual role in regulating stress evolution within the mushy zone, acting both as a source of thermal stress and a path for stress relaxation. Mathematically, the model can be expressed as follows:

$$\begin{cases} \forall x \in [0, x_C], \quad \sigma_{brid}/\sigma_{brid}^{C} < 1, & \text{if} \quad d \le d_C \\ \exists x \in [0, x_C], \quad \sigma_{brid}/\sigma_{brid}^{C} \ge 1, & \text{if} \quad d > d_C \end{cases} \tag{7}$$

where x_C pertains to the point of full coalescence. This expression is completely equivalent to $\sigma_{brid}/\sigma_{brid}^{C}$ for $\forall f_s \in [f_{brid}, 1]$. In other words, when the grain diameter d is less than or equal to the critical grain diameter d_C, cracking will not occur if the ratio of stress accumulated in the solid bridges (σ_{brid}) to strength development of the solid bridges (σ_{brid}^{C}) remains below 1 throughout the solidification interval x. Conversely, when $d > d_C$, cracking will occur if this ratio reaches or exceeds 1 at any point within the interval x.

Using this framework, Liu et al.[173] successfully predicted the HTS of binary Al-Cu, Al-Mg, and Al-Si alloys, effectively capturing the influence of alloy composition, grain size, grain morphology, and cooling rate. The model therefore provides a unified mechanistic interpretation for hot tearing. Despite its novelty, the model also has several limitations and defined boundaries of applicability. First, the assumption that cracks nucleate primarily along solid bridges at dendrite roots makes the model most applicable to dendritic or columnar-grained alloys, whereas its accuracy may diminish for equiaxed or irregular microstructures. Second, this approach requires a large number of physical parameters to

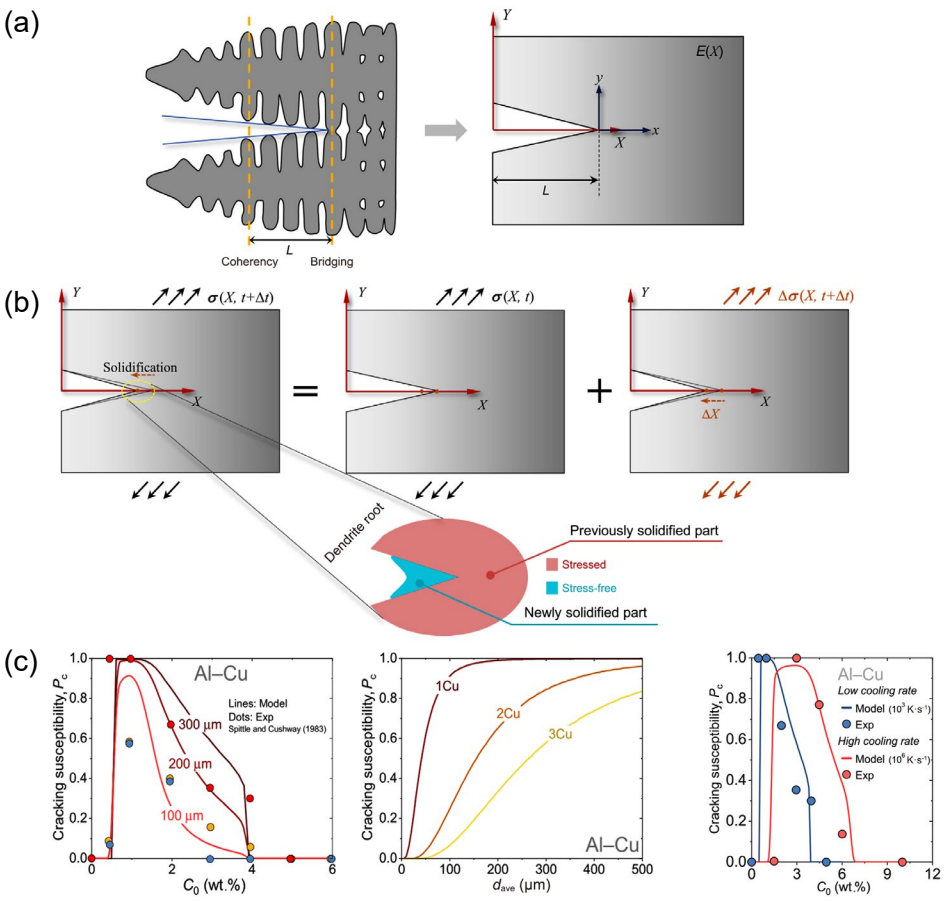

Fig. 14: Liu's model for predicting HTS in Al alloys[173]: (a) crack-like structure of growing dendrites and corresponding simplified model; (b) schematic illustration of a crack model that considers the solidification process; (c) prediction of effects of alloy composition, grain size, and cooling rate on HTS of Al-Cu alloys

be experimentally determined, and different alloy systems need to be individually characterized, which reduces its generalizability. Third, although the model emphasizes the fracture mechanism of solid bridges, other factors such as interdendritic liquid feeding and shrinkage compensation remain critical. Under conditions of high liquid fluidity or steep thermal gradients, liquid flow may significantly influence the cracking process.

6 Summary and future perspectives

This review provides an overview of hot tearing susceptibility (HTS) in cast aluminum (Al) alloys, summarizing the key mechanisms, influencing factors, and recent progress in experimental characterization and predictive criteria. Although substantial advances have been achieved, gaps remain between experimental observations and theoretical models, revealing promising directions for future study:

(1) Advanced characterization and reliable thermophysical data

Future progress depends on acquiring accurate experimental data to support simulations. Traditional post-mortem analyses reveal limited information about dynamic cracking, while many model parameters are still derived under equilibrium assumptions. Synchrotron X-ray imaging now enables the real-time tracking of crack initiation, propagation, and stress evolution during solidification. Such in situ data will greatly improve model fidelity. Given the multiscale nature of solidification, future models should integrate macro-micro coupling with efficient computation and employ temperature-dependent boundary conditions calibrated through experiments[174].

(2) Physically integrated hot tearing criteria

As Eskin[27] noted, a robust criterion should capture the evolution of dominant mechanisms during solidification. Since the RDG criterion, numerous models[175–177] have improved predictive accuracy, yet most still treat liquid feeding and solid deformation independently. Future work should aim to unify these coupled processes, such as feeding control at low solid fractions and plastic deformation at high solid fractions, into a stage-resolved framework. Multi-scale, multi-physics modeling, as demonstrated by Liang et al.[178] for steels, can combine phase-field or cellular automata simulations with finite element and fracture analyses to bridge theory and application.

(3) Data-driven prediction and machine learning

Traditional trial-and-error methods are inefficient for exploring the vast composition-process space. Machine learning (ML) provides an effective alternative for uncovering complex correlations between composition, processing, and HTS. A comprehensive database should include alloy compositions, process parameters, microstructure, and HTS data. Despite challenges in data scarcity and standardization,

data augmentation, transfer learning, and few-shot learning can enhance model reliability. Incorporating thermophysical parameters can also improve the physical interpretability, enabling mechanism-guided alloy design.

(4) Emerging hot tearing mitigation and alloy design strategies

Beyond conventional optimization, new concepts from other alloy systems offer inspiration for mitigating hot tearing. Sun et al.[179] demonstrated that grain boundary segregation in high-entropy alloys can convert tensile stresses to compressive stresses, suppressing hot tearing. Hu et al.[180] developed a liquid-induced healing (LIH) approach using controlled solid-liquid transitions to repair cracks efficiently. These concepts including stress-state engineering and liquid-assisted healing could inspire novel approaches in Al alloys, such as controlled local remelting in eutectic-rich regions to promote microcrack healing and thereby enhance hot tearing resistance.

Acknowledgments

This work was financially supported by the National Natural Science Foundation of China (No. 52475380) and the inaugural Young Elite Scientists Sponsorship Program (Doctoral Student Special Plan) of the China Association for Science and Technology (CAST).

Conflict of interest

Prof. Guo-hua Wu is an EBM of *CHINA FOUNDRY*. He was not involved in the peer-review or handling of this manuscript. The authors have no other competing interests to disclose.

References

[1] Polmear I, John D S, Nie J F, et al. Light alloys: Metallurgy of the light metals. Oxford: Butterworth-Heinemann, 2017: 265–286.
[2] Campbell J. Castings. Oxford: Butterworth-Heinemann, 2003: 267–305.
[3] Flemings M C. Solidification processing. New York: McGraw-Hill, 1974: 12–52.
[4] Kou S. Welding metallurgy. Hoboken: John Wiley and Sons, 2021: 143–338.
[5] Kurz W, Fisher D. Fundamentals of solidification. Switzerland: Trans Tech Publications Ltd., 1998: 1–14.
[6] Eskin D G, Suyitno, Katgerman L. Mechanical properties in the semi-solid state and hot tearing of aluminium alloys. Progress in Materials Science, 2004, 49(5): 629–711.
[7] Li Y, Li H X, Katgerman L, et al. Recent advances in hot tearing during casting of aluminium alloys. Progress in Materials Science, 2021, 117: 100741.
[8] Kubo K, Pehlke R D. Mathematical modeling of porosity formation in solidification. Metallurgical Transactions: B, 1985, 16(2): 359–366.
[9] Song J F, Pan F S, Jiang B, et al. A review on hot tearing of magnesium alloys. Journal of Magnesium and Alloys, 2016, 4(3): 151–172.
[10] Li S, Apelian D. Hot tearing of aluminum alloys: A critical literature review. International Journal of Metalcasting, 2011, 5(1): 23–40.
[11] Sigworth G K. Hot tearing of metals. AFS Transactions, 1996, 155: 1053–1063.
[12] Liu F C, Zhu X Z, Ji S X. Effects of Ni on the microstructure, hot tear and mechanical properties of Al-Zn-Mg-Cu alloys under as-cast condition. Journal of Alloys and Compounds, 2020, 821: 153458.
[13] Pellini W S. Strain theory of hot tearing. Foundry, 1952, 80(11): 125.
[14] Saveiko V N. Theory of hot tearing. Russian Castings Production, 1961, 11: 453–456.
[15] Borland J C. Fundamentals of solidification cracking in welds. Welding and Metal Fabrication, 1979, 3: 99–107.
[16] Zhong H G, Zhao Y, Lin Z H, et al. Understanding the roles of interdendritic bridging on hot tearing formation during alloy solidification. Journal of Materials Research and Technology, 2023, 27: 5368–5371.
[17] Bai S W, Wang F, Du X D, et al. Reduced hot tearing susceptibility of Mg-4Zn-1.5Ca-*x*Y-0.3Zr alloy by introducing intergranular bridging secondary phases. Journal of Alloys and Compounds, 2025, 1014: 178663.
[18] Zhou R, Fang X G, Zhang K X, et al. Relationship between characteristics of liquid film and hot tearing phenomena during solidification of hypereutectic Al-Si alloy. Journal of Materials Science, 2025, 60: 6987–7001.
[19] Clyne T W, Wolf M, Kurz W. The effect of melt composition to continuous casting. Metallurgical Transactions, 1982, 13: 259.
[20] Clyne T W, Davies G J. A quantitative solidification cracking test for castings and an evaluation of cracking in Al-Mg alloys. British Foundryman, 1975, 68(9): 238–244.
[21] Chen Y Q, Liu Z, Liu S M, et al. Effect of Cu on the hot tearing susceptibility of Al-6Zn-2.5Mg-*x*Cu alloy. International Journal of Metalcasting, 2021, 15(1): 130–140.
[22] Beeley P. Solidification 2: The feeding of castings. Foundry Technology, 2nd ed., Oxford: Butterwoth-Heinemann, 2001: 100–177. https://doi.org/10.1016/B978-075064567-6/50006-6
[23] Zhang X B, Li D, Zeng L, et al. Effect of SiC particles content on the hot tearing susceptibility of SiC/Al_5Cu composites. Ceramics International, 2020, 46(8): 10610–10618.
[24] Xu R F, Zheng H L, Luo J, et al. Role of tensile forces in hot tearing formation of cast Al-Si alloy. Transactions of Nonferrous Metals Society of China, 2014, 24(7): 2203–2207.
[25] Durman M, Murphy S. An improved parametric pressure-die-cast zinc-based alloy. Zeitschrift Fur Metallkde, 1991, 82: 129.
[26] Nabawy A M, Samuel A M, Doty H W, et al. A review on the criteria of hot tearing susceptibility of aluminum cast alloys. International Journal of Metalcasting, 2021, 15(4): 1362–1374.
[27] Eskin D G, Katgerman L. A quest for a new hot tearing criterion. Metallurgical and Materials Transactions: A, 2007, 38(7): 1511–1519.
[28] Liu J W, Kou S. Crack susceptibility of binary aluminum alloys during solidification. Acta Materialia, 2016, 110: 84–94.
[29] Han Q. A model correlating fluidity to alloy variables in hypoeutectic alloys. Acta Materialia, 2022, 226: 117587.
[30] Ravi K R, Pillai R M, Amaranathan K R, et al. Fluidity of aluminum alloys and composites: A review. Journal of Alloys and Compounds, 2008, 456(1–2): 201–210.
[31] Hu B, Li D J, Li Z X, et al. Hot tearing behavior in double ternary eutectic alloy system: Al-Mg-Si alloys. Metallurgical and Materials Transactions: A, 2021, 52(2): 789–805.
[32] Hu B, Li D J, Wang J Y, et al. Hot tearing behavior in double ternary eutectic alloy system: Mg-Ce-Al alloys. Metallurgical and Materials Transactions: A, 2020, 51(12): 6658–6669.
[33] Liu J W, Kou S. Susceptibility of ternary aluminum alloys to cracking during solidification. Acta Materialia, 2017, 125: 513–523.

[34] Liu J W, Zeng P W, Kou S. Solidification cracking susceptibility of quaternary aluminium alloys. Science and Technology of Welding and Joining, 2021, 26(3): 244–257.
[35] Han J Q, Wang J S, Zhang M S, et al. Susceptibility of lithium containing aluminum alloys to cracking during solidification. Materialia, 2019, 5: 100203.
[36] Guo Y J, Li J F, Lu D D, et al. Characterization of Al_3Zr precipitation via double-step homogenization and recrystallization behavior after subsequent deformation in 2195 Al-Li alloy. Materials Characterization, 2021, 182: 111549.
[37] Dasgupta S, Kou S. Undercooling and cracking during solidification. Metallurgical and Materials Transactions: A, 2024, 55(9): 3450–3462.
[38] Liu J W, Kou S. Effect of diffusion on susceptibility to cracking during solidification. Acta Materialia, 2015, 100: 359–368.
[39] Geng S N, Jiang P, Shao X Y, et al. Effects of back-diffusion on solidification cracking susceptibility of Al-Mg alloys during welding: A phase-field study. Acta Materialia, 2018, 160: 85–96.
[40] Geng S N, Jiang P, Shao X Y, et al. Comparison of solidification cracking susceptibility between Al-Mg and Al-Cu alloys during welding: A phase-field study. Scripta Materialia, 2018, 150: 120–124.
[41] Liu J W, Duarte H P, Kou S. Evidence of back diffusion reducing cracking during solidification. Acta Materialia, 2017, 122: 47–59.
[42] Kou S. Dihedral angle and cracking during solidification. Metallurgical and Materials Transactions: A, 2025, 56(3): 1024–1036.
[43] Kou S. Grain refining and cracking during solidification. Metallurgical and Materials Transactions: A, 2024, 55(11): 4663–4675.
[44] Wang L, Wang N, Provatas N. Liquid channel segregation and morphology and their relation with hot cracking susceptibility during columnar growth in binary alloys. Acta Materialia, 2017, 126: 302–312.
[45] Yue C Y, Yuan X G, Su M, et al. Effect of adding Pr on the microstructure and hot tearing sensitivity of as-cast Al-Cu-Mg alloys. Materials Characterization, 2022, 191: 112141.
[46] Zhang X B, Zhu P, Zeng L, et al. Effect of adding Ce on the hot-tearing susceptibility of the $5TiB_2$/Al-5Cu composite. Materials Characterization, 2020, 168: 110552.
[47] Wang Y X, Yue C Y, Su M, et al. Effect of Ce on hot tearing sensitivity of as-cast Al-Cu-Mg-Y alloy. Journal of Materials Engineering and Performance, 2022, 31(8): 6349–6359.
[48] Tao C C, Huang H J, Yuan X G, et al. Effect of Y element on microstructure and hot tearing sensitivity of as-cast Al-4.4Cu-1.5Mg-0.15Zr alloy. International Journal of Metalcasting, 2021, 16(2): 1010–1019.
[49] Yue C Y, Zheng B W, Su M, et al. Effect of Y and Ce micro-alloying on microstructure and hot tearing of as-cast Al-Cu-Mg alloy. Acta Metallurgica Sinica (English Letters), 2024, 37(6): 939–952.
[50] Benoit M J, Zhu S M, Abbott T B, et al. Evaluation of the effect of rare earth alloying additions on the hot tearing susceptibility of aluminum alloy 7150 during rapid solidification. Metallurgical and Materials Transactions: A, 2020, 51(10): 5213–5227.
[51] Li M, Wang H W, Wei Z J, et al. The effect of Y on the hot-tearing resistance of Al-5 wt.% Cu based alloy. Materials & Design, 2010, 31(5): 2483–2487.
[52] Opprecht M, Garandet J P, Roux G, et al. A solution to the hot cracking problem for aluminium alloys manufactured by laser beam melting. Acta Materialia, 2020, 197: 40–53.
[53] Li R D, Wang M B, Li Z M, et al. Developing a high-strength Al-Mg-Si-Sc-Zr alloy for selective laser melting: Crack-inhibiting and multiple strengthening mechanisms. Acta Materialia, 2020, 193: 83–98.
[54] Lin S, Aliravci C, Pekguleryuz M O. Hot-tear susceptibility of aluminum wrought alloys and the effect of grain refining. Metallurgical and Materials Transactions: A, 2007, 38(5): 1056–1068.
[55] Xu Y T, Zhang Z F, Gao Z H, et al. Effect of Sc on the hot cracking properties of 7xxx aluminum alloy and the microstructure of squeeze castings. Materials, 2021, 14(22): 6881.
[56] Puparattanapong K, Pandee P, Boontein S, et al. Fluidity and hot cracking susceptibility of A356 alloys with Sc additions. Transactions of the Indian Institute of Metals, 2018, 71(7): 1583–1593.
[57] Sokoluk M, Cao C Z, Pan S H, et al. Nanoparticle-enabled phase control for arc welding of unweldable aluminum alloy 7075. Nature Communications, 2019, 10(1): 98.
[58] Choi H, Cho W H, Konishi H, et al. Nanoparticle-induced superior hot tearing resistance of A206 alloy. Metallurgical and Materials Transactions: A, 2013, 44(4): 1897–1907.
[59] Li S M, Sadayappan K, Apelian D. Role of grain refinement in the hot tearing of cast Al-Cu alloy. Metallurgical and Materials Transactions: B, 2013, 44(3): 614–623.
[60] Bai Q L, Li Y, Li H X, et al. Roles of alloy composition and grain refinement on hot tearing susceptibility of 7××× aluminum alloys. Metallurgical and Materials Transactions: A, 2016, 47(8): 4080–4091.
[61] Sigworth G K. Grain refining of aluminum casting alloys: Unsolved mysteries. International Journal of Metalcasting, 2024, 45(3): 1–30.
[62] Razaz G, Carlberg T. Hot tearing susceptibility of AA3000 aluminum alloy containing Cu, Ti, and Zr. Metallurgical and Materials Transactions: A, 2019, 50(8): 3842–3854.
[63] Li Y, Bai Q L, Liu J C, et al. The influences of grain size and morphology on the hot tearing susceptibility, contraction, and load behaviors of AA7050 alloy inoculated with Al-5Ti-1B master alloy. Metallurgical and Materials Transactions: A, 2016, 47(8): 4024–4037.
[64] Li P F, Sui Y D, Jiang Y H, et al. Optimizing hot tearing susceptibility of Al-5.5Zn-2.4 Mg-1.3Cu alloys by grain refinement, increasing mold and casting temperature. Materials & Design, 2024, 246: 113325.
[65] Li S M, Sadayappan K, Apelian D. Effects of mold temperature and pouring temperature on the hot tearing of cast Al-Cu alloys. Metallurgical and Materials Transactions: B, 2016, 47(5): 2979–2990.
[66] Wang Y X, Wu G H, Zhang L, et al. Effect of pouring and mold temperatures on fluidity and hot tearing behavior of cast Al-Li-Cu-Mg-Sc-Zr-Ti alloy. Transactions of Nonferrous Metals Society of China, 2025, 35(3): 669–683.
[67] Song J F, Wang Z, Huang Y D, et al. Effect of Zn addition on hot tearing behaviour of Mg-0.5Ca-xZn alloys. Materials & Design, 2015, 87: 157–170.
[68] Coniglio N, Cross C E. Mechanisms for solidification crack initiation and growth in aluminum welding. Metallurgical and Materials Transactions: A, 2009, 40(11): 2718–2728.
[69] Guo Y J, Zhang L, Wu G H, et al. Effect of Li content on hot tearing susceptibility of ternary Al-Cu-Li alloys: Experimental investigation, criterion prediction and simulation assessment. Metallurgical and Materials Transactions: A, 2023, 54(12): 4850–4867.
[70] Guo Y J, Zhang L, Wu G H, et al. Influence of Cu addition on hot tearing susceptibility and fluidity of Al-Li-Cu alloys: Experimental investigation, criterion prediction and simulation assessment. Journal of Alloys and Compounds, 2023, 969: 172301.
[71] Guo Y J, Qi F Z, Zhang L, et al. Achieving low hot tearing susceptibility in high-strength cast Al-Li alloys: Experimental investigation and simulation assessment. Materials Science & Engineering: A, 2024, 910: 146901.

[72] Guo Y J, Qi F Z, Zhang L, et al. Unveiling the origin of severe hot cracking susceptibility in Al-Li alloys. Materials Letters, 2024, 367: 136606.
[73] Guo Y J, Qi F Z, Wang Y H, et al. An extended criterion for hot cracking susceptibility of Al-Li alloys. Engineering Failure Analysis, 2025, 171: 109348.
[74] Ahmad M. Thermal oxidation behavior of an Al-Li-Cu-Mg-Zr alloy. Metallurgical Transactions: A, 1987, 18(4): 681–689.
[75] Xu Y C, Li G Y, Jiang W M, et al. Significant elimination of pore defect and interfacial reaction of sand casted Al-Li alloy castings via a novel inorganic binder coating. Journal of Materials Research and Technology, 2022, 21: 4360–4371.
[76] Xu Y C, Li G Y, Jiang W M, et al. Investigation on characteristic and formation mechanism of porosity defects of Al-Li alloys prepared by sand casting. Journal of Materials Research and Technology, 2022, 19: 4063–4075.
[77] Noble B, Harris S J, Dinsdale K. The elastic modulus of aluminium-lithium alloys. Journal of Materials Science, 1982, 17(2): 461–468.
[78] Pickens J R. The weldability of lithium-containing aluminium alloys. Journal of Materials Science, 1985, 20(12): 4247–4258.
[79] Mukherjee D, Sahoo B D, Joshi K D, et al. Thermo-physical properties of LiH at high pressures by *ab initio* calculations. Journal of Applied Physics, 2011, 109(10): 103515.
[80] Leitner M, Leitner T, Schmon A, et al. Thermophysical properties of liquid aluminum. Metallurgical and Materials Transactions: A, 2017, 48(6): 3036–3045.
[81] Bai X R, Xie H N, Zhang X, et al. Heat-resistant super-dispersed oxide strengthened aluminium alloys. Nature Materials, 2024, 23(6): 747–754.
[82] Partridge P G. Oxidation of aluminium-lithium alloys in the solid and liquid states. International Materials Reviews, 1990, 35(1): 37–58.
[83] Hull S, Farley T W D, Hayes W, et al. The elastic properties of lithium oxide and their variation with temperature. Journal of Nuclear Materials, 1988, 160(2–3): 125–134.
[84] Billone M C, Liu Y Y, Poeppel R B, et al. Elastic and creep properties of Li_2O. Journal of Nuclear Materials, 1986, 141–143: 282–288.
[85] Puncreobutr C, Lee P D, Kareh K M, et al. Influence of Fe-rich intermetallics on solidification defects in Al-Si-Cu alloys. Acta Materialia, 2014, 68: 42–51.
[86] Dong H, Wang F, Wang Z, et al. Effect of Sn addition on hot tearing susceptibility of AXJ530 alloy. Materials Research Express, 2018, 5(3): 036513.
[87] Du X, Wang F, Wang Z, et al. Hot tearing susceptibility of AXJ530 alloy under low-frequency alternating magnetic field. Acta Metallurgica Sinica (English Letters), 2020, 33(9): 1259–1270.
[88] Li B C, Zhang J, Ye F W, et al. An approach to studying the hot tearing mechanism of alloying elements in ternary Mg-Zn-Al alloys. Journal of Materials Processing Technology, 2023, 317: 117980.
[89] Kang B K, Sohn I. Effects of Cu and Si contents on the fluidity, hot tearing, and mechanical properties of Al-Cu-Si alloys. Metallurgical and Materials Transactions: A, 2018, 49(10): 5137–5145.
[90] Li P F, Sui Y D, Shen W, et al. High content of solute elements (Zn, Mg, Cu) increases the hot tearing susceptibility resistance of Al-Zn-Mg-Cu alloys. Journal of Alloys and Compounds, 2025, 1022: 179852.
[91] Wang Y S, Wang Q D, Wu G H, et al. Hot-tearing susceptibility of Mg-9Al-*x*Zn alloy. Materials Letters, 2002, 57: 929–934.
[92] Cao G, Kou S. Hot tearing of ternary Mg-Al-Ca alloy castings. Metallurgical and Materials Transactions: A, 2006, 37(12): 3647–3663.
[93] Li S S, Tang B, Jin X Y, et al. An investigation on hot-cracking mechanism of Sr addition into Mg-6Al-0.5Mn alloy. Journal of Materials Science, 2012, 47(4): 2000–2004.
[94] Cao G, Haygood I, Kou S. Onset of hot tearing in ternary Mg-Al-Sr alloy castings. Metallurgical and Materials Transactions: A, 2010, 41(8): 2139–2150.
[95] Hamadellah A, Bouayad A, Gerometta C. Hot tear characterization of AlCu5MgTi and AlSi9 casting alloys using an instrumented constrained six rods casting method. Journal of Materials Processing Technology, 2017, 244: 282–288.
[96] Li B C, Zhang J, Dong Q, et al. New insights into hot tearing mechanisms of alloying elements based on ternary Mg-Gd-Y alloys. Engineering Failure Analysis, 2024, 162: 108384.
[97] Wei Z Q, Yang S Y, Gu H Y, et al. Study of hot tearing susceptibility and crack arrest mechanism of Mg-Y-Ni alloys containing LPSO structure. Engineering Failure Analysis, 2025, 177: 109678.
[98] Su M, Zheng W T, Fu D K, et al. Design and application of a multichannel “cross” hot tearing tendency device: A study on hot tearing tendency of Al alloys. China Foundry, 2022, 19(4): 327–334.
[99] Yue C Y, Zheng B W, Su M, et al. Effect of Cu/Mg ratio on the intermetallic compound and hot tearing susceptibility of Al-Cu-Mg alloys. International Journal of Metalcasting, 2024, 18(1): 417–430.
[100] Li S, Apelian D, Sadayappan K. Hot tearing in cast Al alloys: Mechanisms and process controls. International Journal of Metalcasting, 2012, 6(3): 51–58.
[101] Song J F, Zhao H, Liao J G, et al. Comparison on hot tearing behavior of binary Mg-Al, Mg-Y, Mg-Gd, Mg-Zn, and Mg-Ca alloys. Metallurgical and Materials Transactions: A, 2022, 53(8): 2986–3001.
[102] Hu B, Li D J, Li Z X, et al. Step-by-step observation of secondary-phase evolution during the casting cracking process in Mg-Ce-Al alloys. Metallurgical and Materials Transactions: A, 2022, 53(9): 3478–3492.
[103] Zhao H, Song J F, Wang J, et al. Semi-solid tensile behavior and its relationship with hot tearing susceptibility of Mg-*x*Ca alloys. International Journal of Metalcasting, 2024, 18(2): 1119–1134.
[104] Davidson C, Viano D, Lu L, et al. Observation of crack initiation during hot tearing. International Journal of Cast Metals Research, 2013, 19(1): 59–65.
[105] Haaften W M V, Kool W H, Katgerman L. Hot tearing studies in AA5182. Journal of Materials Engineering and Performance, 2002, 11(5): 537–543.
[106] D’Elia F, Ravindran C, Sediako D, et al. Hot tearing mechanisms of B206 aluminum-copper alloy. Materials & Design, 2014, 64: 44–55.
[107] D’Elia F, Ravindran C, Sediako D. Interplay among solidification, microstructure, residual strain and hot tearing in B206 aluminum alloy. Materials Science & Engineering: A, 2015, 624: 169–180.
[108] Fan X Q, Fleming T G, Clark S J, et al. Magnetic modulation of keyhole instability during laser welding and additive manufacturing. Science, 2025, 387(6736): 864–869.
[109] Ioannidou C, König H H, Semjatov N, et al. In-situ synchrotron X-ray analysis of metal additive manufacturing: Current state, opportunities and challenges. Materials & Design, 2022, 219: 110790.
[110] Chen Y H, Zhang D Y, O’Toole P, et al. In situ observation and reduction of hot-cracks in laser additive manufacturing. Communications Materials, 2024, 5(1): 84.
[111] Guo L P, Liu H J, Tang Z J, et al. Fluid flow and bubble evolution in the melt pool of high-power (>2500 W) laser additive manufacturing of aluminum captured by X-ray imaging. Transactions of Materials Research, 2025, 1: 100084.

[112] Liotti E, Lui A, Connolley T, et al. Probing interdendritic flow and hot tearing during solidification using real time X-ray imaging and droplet tracking. Acta Materialia, 2022, 240: 118298.
[113] Rees D T, Leung C L A, Elambasseril J, et al. In situ X-ray imaging of hot cracking and porosity during LPBF of Al-2139 with TiB_2 additions and varied process parameters. Materials & Design, 2023, 231: 112031.
[114] Phillion A B, Hamilton R W, Fuloria D, et al. In situ X-ray observation of semi-solid deformation and failure in Al-Cu alloys. Acta Materialia, 2011, 59(4): 1436–1444.
[115] Han I, Feng S K, Wilde F, et al. Revealing hot tear formation dynamics in Al-Cu alloys with X-ray radiography. Acta Materialia, 2024, 262: 119421.
[116] Li X X, Wang J S, Miao Y S, et al. In-situ study on the effect of Li concentration on hydrogen microporosity evolution in Al-Li alloys by synchrotron X-ray radiography. Journal of Alloys and Compounds, 2024, 1008: 176810.
[117] Wu Z K, Wu S C, Kruzic J J, et al. Critical damage events of 3D printed AlSi10Mg alloy via in situ synchrotron X-ray tomography. Acta Materialia, 2025, 282: 120464.
[118] Terzi S, Salvo L, Sue´ry M, et al. In situ X-ray tomography observation of inhomogeneous deformation in semi-solid aluminium alloys. Scripta Materialia, 2009, 61(5): 449–452.
[119] Phillion A B, Cockcroft S L, Lee P D. X-ray micro-tomographic observations of hot tear damage in an Al-Mg commercial alloy. Scripta Materialia, 2006, 55(5): 489–492.
[120] Puncreobutr C, Lee P D, Hamilton R W, et al. Synchrotron tomographic characterization of damage evolution during aluminum alloy solidification. Metallurgical and Materials Transactions: A, 2013, 44(12): 5389–5395.
[121] Xiang K, Qin L, Zhao Y L, et al. Operando study of the dynamic evolution of multiple Fe-rich intermetallics of an Al recycled alloy in solidification by synchrotron X-ray and machine learning. Acta Materialia, 2024, 279: 120267.
[122] Zhao Y, Du W, Koe B, et al. 3D characterisation of the Fe-rich intermetallic phases in recycled Al alloys by synchrotron X-ray microtomography and skeletonisation. Scripta Materialia, 2018, 146: 321–326.
[123] Shao L X, Li X F, Zhao G P, et al. Synergistic effect of in situ TiB_2 particle and Ti solute on fluidity and hot tearing susceptibility of Al-Li-Cu-*X* alloy. Journal of Materials Science, 2024, 59(37): 17666–17687.
[124] Shao L X, Li X F, Zhao G P, et al. Experimental investigation and simulation assessment on fluidity and hot tearing susceptibility of Al-Li-Cu-*X* alloy: The role of microalloying elements. Materials Characterization, 2024, 218: 114469.
[125] Han J Q, Wang J S, Zhang M S, et al. Relationship between amounts of low-melting-point eutectics and hot tearing susceptibility of ternary Al-Cu-Mg alloys during solidification. Transactions of Nonferrous Metals Society of China, 2020, 30(9): 2311–2325.
[126] Zhou Y, Mao P L, Wang Z, et al. Experimental investigation and simulation assessment on fluidity and hot tearing of Mg-Zn-Cu system alloys. Journal of Materials Processing Technology, 2021, 297: 17259.
[127] Wang K, Fu P H, Peng L M, et al. A simplified hot-tearing criterion for shape castings based on temperature-field simulation. Metallurgical and Materials Transactions: A, 2019, 50(11): 5271–5280.
[128] Zhu Y K, Zhou K K, Xu G Q, et al. Crack formation of camshaft castings: Hot tearing susceptibility and root causes. Engineering Failure Analysis, 2023, 147: 107143.
[129] Du X D, Wang F, Wang Z, et al. Effect of Ca/Al ratio on hot tearing susceptibility of Mg-Al-Ca alloy. Journal of Alloys and Compounds, 2022, 911: 165113.
[130] Sheykh-jaberi F, Cockcroft S L, Maijer D M, et al. Meso-scale modelling of semi-solid deformation in aluminum foundry alloys: Effects of feeding and microstructure on hot tearing susceptibility. Journal of Materials Processing Technology, 2020, 279: 116551.
[131] Wang Y H, Guo Y J, Zhao D C, et al. Evaluation of Cu content on mechanical performance and castability of AlMg5.4Si2 alloy. Journal of Alloys and Compounds, 2024, 1002: 175539.
[132] Phillion A B, Cockcroft S L, Lee P D. A three-phase simulation of the effect of microstructural features on semi-solid tensile deformation. Acta Materialia, 2008, 56(16): 4328–4338.
[133] Sistaninia M, Phillion A B, Drezet J M, et al. Simulation of semi-solid material mechanical behavior using a combined discrete/finite element method. Metallurgical and Materials Transactions: A, 2011, 42(1): 239–248.
[134] Su T C, O'Sullivan C, Nagira T, et al. Semi-solid deformation of Al-Cu alloys: A quantitative comparison between real-time imaging and coupled LBM-DEM simulations. Acta Materialia, 2019, 163: 208–225.
[135] Takai R, Endo N, Hirohara R, et al. Experimental and numerical analysis of grain refinement effect on hot tearing susceptibility for Al-Mg alloys. The International Journal of Advanced Manufacturing Technology, 2019, 100: 1867–1880.
[136] Sistaninia M, Phillion A B, Drezet J M, et al. A 3-D coupled hydromechanical granular model for simulating the constitutive behavior of metallic alloys during solidification. Acta Materialia, 2012, 60(19): 6793–6803.
[137] Liu J W, Hu P F, Kou S. A CFD study on intergranular liquid feeding and cracking during solidification in welding. Metallurgical and Materials Transactions: A, 2023, 54(11): 4342–4355.
[138] Wang W Y, Shang S L, Fang H Z, et al. Effects of composition on atomic structure, diffusivity, and viscosity of liquid Al-Zr alloys. Metallurgical and Materials Transactions: A, 2012, 43(10): 3471–3480.
[139] Wang W Y, Han J J, Fang H Z, et al. Anomalous structural dynamics in liquid $Al_{80}Cu_{20}$: An *ab initio* molecular dynamics study. Acta Materialia, 2015, 97: 75-85.
[140] Su M, Yuan X G, Yue C Y, et al. Influence of liquid film characteristics on hot cracking initiation in Al-Cu alloys at the end of solidification. Acta Metallurgica Sinica (English Letters), 2023, 36(1): 103–117.
[141] Roik O S, Samsonnikov O V, Kazimirov V P, et al. Medium-range order in Al-based liquid binary alloys. Journal of Molecular Liquids, 2010, 151(1): 42–49.
[142] Su M, Zhou M H, Yue C Y, et al. Investigation on the influence mechanism of Mg contents on the hot cracking behavior of Al-Cu-Mg alloys. Metallurgical and Materials Transactions: B, 2024, 56(1): 355–374.
[143] Su M, Yuan X G, Yue C Y, et al. Effect of liquid film constitutional supercooling at the end of solidification on the hot cracking behavior of Al-4.0 wt.%Cu alloy. Materials Letters, 2022, 328: 133116.
[144] Zhang Y F, Su M. Improvements of hot cracking in Al-Cu alloys – The positive effect of alloying on the liquid film feeding capacity. Materials Letters, 2025, 396: 138774.
[145] Zhang Y F, Su M. Hot cracking in Al-Cu-Mg alloys – Effects of liquid film characteristics and intermetallic compounds. Journal of Alloys and Compounds, 2025, 1027: 180485.
[146] Li L F, Zhang R J, Yuan Q Q, et al. An integrated approach to study the hot tearing behavior by coupling the microscale phase field model and macroscale casting simulations. Journal of Materials Processing Technology, 2022, 310: 117782.
[147] Yang L S, Yang J, Han F, et al. Hot cracking susceptibility prediction from quantitative multi-phase field simulations with grain boundary effects. Acta Materialia, 2023, 250: 118821.

[148] Ma C Z, Zhang R J, Li Z X, et al. Effects of solidification shrinkage on solute segregation and hot cracking sensitivity in liquid channel during columnar dendrite growth. Journal of Materials Research and Technology, 2024, 31: 2367–2375.
[149] Chen D X, Wang J S, Zhang C. Coupling phase-field model and CFD for hot cracking predictions of Al-Li alloys. Computational Materials Science, 2021, 192: 110361.
[150] Feurer U. Quality control of engineering alloys and the role of metals science. Delft: Delft University of Technology, 1977: 260–289.
[151] Clyne T W, Davies G J. Solidification and casting of metals. London: Metals Society, 1979: 235–268.
[152] Clyne T W, Davies G J. The influence of composition on solidification cracking susceptibility in binary alloy systems. British Foundryman, 1981, 74: 65–73.
[153] Katgerman L. A mathematical model for hot cracking of aluminum alloys during D.C. casting. JOM, 1982, 34(2): 46–49.
[154] Rappaz M, Drezet J M, Gremaud M. A new hot-tearing criterion. Metallurgical and Materials Transactions: A, 1999, 30(2): 449–455.
[155] Li Y, Gao X, Zhang Z R, et al. Experimental and theoretical studies of the hot tearing behavior of Al-xZn-2Mg-2Cu alloys. Metallurgical and Materials Transactions: A, 2017, 48(10): 4744–4754.
[156] Guo Y J, Wang Y H, Qi F Z, et al. Enhancing solidification cracking resistance in high-strength Al-Li alloys via strategic light rare earth alloying: An integrated experiment-simulation approach. Materials & Design, 2025, 259: 114826.
[157] Braccini M, Martin C L, Suery M, et al. Modeling of casting, welding and advanced solidification processes IX. Aachen: Shaker Verlag GmbH, 2000: 1–126.
[158] Grandfield J F, Davidson C J, Taylor J A. Application of a new hot tearing analysis to horizontal direct chili cast magnesium alloy AZ91. Light Metals, 2001: 895–901.
[159] Zhang Z H, Yang L S, Wang H, et al. A permeability model for hot cracking susceptibility prediction across near-equilibrium to rapid solidification conditions. Journal of Materials Research and Technology, 2025, 36: 6902–6910.
[160] Suyitno, Kool W H, Katgerman L. Integrated approach for prediction of hot tearing. Metallurgical and Materials Transactions: A, 2009, 40(10): 2388–2400.
[161] Griffith A A. The phenomena of rupture and flow in solids. Philosophical Transactions of the Royal Society of London, 1920, 221: 163–167.
[162] Margolin L G. A generalized Griffith criterion for crack propagation. Engineering Fracture Mechanics, 1984, 19(3): 539–543.
[163] Li Y, Zhang Z R, Zhao Z Y, et al. Effect of main elements (Zn, Mg, and Cu) on hot tearing susceptibility during direct-chill casting of 7xxx aluminum alloys. Metallurgical and Materials Transactions: A, 2019, 50(8): 3603–3616.
[164] Bai Q L, Liu J C, Li H X, et al. A modified hot tearing criterion for direct chill casting of aluminium alloys. Materials Science and Technology, 2016, 32(8): 846–854.
[165] Sistaninia M, Phillion A B, Drezet J M, et al. Three-dimensional granular model of semi-solid metallic alloys undergoing solidification: Fluid flow and localization of feeding. Acta Materialia, 2012, 60(9): 3902–3911.
[166] Sistaninia M, Terzi S, Phillion A B, et al. 3-D granular modeling and in situ X-ray tomographic imaging: A comparative study of hot tearing formation and semi-solid deformation in Al-Cu alloys. Acta Materialia, 2013, 61(10): 3831–3841.
[167] Rajani H R Z, Phillion A B. 3D multi-scale multi-physics modelling of hot cracking in welding. Materials & Design, 2018, 144: 45–54.
[168] Kou S. A criterion for cracking during solidification. Acta Materialia, 2015, 88: 366–374.
[169] Hu B, Li Z X, Li D J, et al. A hot tearing criterion based on solidification microstructure in cast alloys. Journal of Materials Science & Technology, 2022, 105: 68–80.
[170] Tang G N, Gould B J, Ngowe A, et al. An updated index including toughness for hot-cracking susceptibility. Metallurgical and Materials Transactions: A, 2022, 53(4): 1486–1498.
[171] Liu J W, Hu P F, Kou S. An axisymmetric analytical model for cracking during solidification and its comparison with the RDG model. Metallurgical and Materials Transactions: A, 2024, 55: 1435–1447.
[172] Su M, Zheng W T, Yue C Y, et al. A hot cracking initiation criterion based on solidification liquid film characteristic and microstructure. Acta Metallurgica Sinica (English Letters), 2023, 36: 1776–1790.
[173] Liu W B, Li G, Lu J. Modeling solidification cracking: A new perspective on solid bridge fracture. Journal of the Mechanics and Physics of Solids, 2024, 188: 105651.
[174] Jolly M, Katgerman L. Modelling of defects in aluminium cast products. Progress in Materials Science, 2022, 123: 100824.
[175] Pujiyulianto E, Suyitno, Rajagukguk K, et al. Effect of chemical composition on hot cracking susceptibility (HCS) using various hot cracking criteria. Engineering Failure Analysis, 2023, 152: 107501.
[176] Suyitno, Kool W H, Katgerman L. Hot tearing criteria evaluation for direct-chill casting of an Al-4.5 pct Cu alloy. Metallurgical and Materials Transactions: A, 2005, 36: 1537–1546.
[177] Liu Y Q, Zhi X Y, Gao Z M, et al. The physical model of hot tearing based on formation of microporosity in aluminum alloys. Journal of Materials Research and Technology, 2025, 38: 451–457.
[178] Liang X H, Agarwal G, Hermans M, et al. A multi-scale modeling framework for solidification cracking during welding. Acta Materialia, 2025, 283: 120530.
[179] Sun Z J, Tan X P, Wang C C, et al. Reducing hot tearing by grain boundary segregation engineering in additive manufacturing: Example of an $Al_xCoCrFeNi$ high-entropy alloy. Acta Materialia, 2021, 204: 116505.
[180] Hu X G, Guo C, Huang Y H, et al. Liquid-induced healing of cracks in nickel-based superalloy fabricated by laser powder bed fusion. Acta Materialia, 2024, 267: 119731.